Table 1. Comparison of the tumorigenicity-associated assays.

Assay	Soft agar colony formation assay	Flow cytometry	qRT-PCR	*In vivo* tumorigenicity assay using SCID mice (Reference #11)
Measurement standard	Colony formation	Expression of marker protein for pluripotency	Expression of marker gene for pluripotency	Tumor formation
Purpose	Detection of anchorage independent growth	Detection of undifferentiated pluripotent cells	Detection of undifferentiated pluripotent cells	Detection of tumorigenic or undifferentiated pluripotent cells
Time	30 days	1 day	6 hours	12–16 weeks
Advantage	Inexpensive	Rapid	Rapid and simple	Direct
		Analyzing individual cells	Quantitative	Analyzing tumor formation in a specific microenvironment
			High sensitivity	
Disadvantage	Indirect	Indirect	Indirect	Costly
	Not applicable to hiPSCs	Detecting only the cells that express the known maker molecules	Detecting only the cells that express the known marker genes	Time-consuming
		Gating techniques strongly influence the result		
LLOD	1% of PA-1	0.1% of hiPSC (TRA-1-60)	=<0.002% of hiPSC* (Lin28)	245 undifferentiated hESCs with 10^6 feeder fibroblasts (0.025%)

*Not based on the calculation found in Reference #21 because the background signal from the negative controls (primary RPE cells) was not detectable.
doi:10.1371/journal.pone.0037342.t001

qRT-PCR

Total RNA was isolated from cell cultures using an RNeasy Mini Kit (Qiagen, Hilden, Germany) and treated with DNase I according to the manufacturer's instructions. In the spike study, 201B7 cells and RPE cells were mixed at a defined cell number, before total RNA isolation. qRT-PCR was performed with the QuantiTect Probe one-step RT-PCR Kit (Qiagen) on a 7300 Real-Time PCR System (Applied Biosystems, Foster City, CA). The expression levels of target genes were normalized to those of the GAPDH (glyceraldehyde-3-phosphate dehydrogenase) transcript, which were quantified using TaqMan human GAPDH control reagents (Applied Biosystems). Probes and primers were obtained from Sigma–Aldrich. The sequences of primers and probes used in the present study are listed in Table S1. All qRT-PCR reactions were run at 45 cycles.

Flow Cytometry

201B7 cells and RPE cells were dissociated into single cells as described above. Cells were fixed with the BD Cytofix fixation buffer (BD Biosciences, Bedford, MA) for 20 min and permeabilized with BD Perm/Wash buffer (BD Biosciences) for 10 min at room temperature. Cells were incubated for 1 h at room temperature with the following primary antibodies and fluorochrome-conjugated antibodies: mouse anti-CRALBP monoclonal 1:1000 (B2, Thermo Scientific, Roskilde, Denmark); rabbit anti-GP-100 monoclonal 1:1000 (P14-V, Enzo Life Sciences, Lausen, Switzerland); FITC mouse anti-TRA-1-60 monoclonal 1:5 (TRA-1-60, BD Pharmingen); PE mouse anti-TRA-1-81 monoclonal 1:5 (TRA-1-81, BD Pharmingen); PerCP-Cy5.5 mouse anti-Oct3/4 monoclonal 1:5 (40/Oct-3, BD Pharmingen); Alexa Fluor 647 mouse anti-Sox2 monoclonal 1:5 (245610, BD Pharmingen); PE mouse anti-Nanog monoclonal 1:5 (N31–355, BD Pharmingen). Indirect immunostaining was then completed with either donkey-anti-mouse or donkey-anti-rabbit Alexa Fluor 647-conjugated secondary antibodies 1:1000 (Molecular Probes) for 1 h. Appropriate antibodies were used as a negative control. To obtain fluorescein-labeled hiPSCs, 201B7 cells were incubated with 10 μM carboxyfluorescein diacetate succinimidyl ester (CFDA; Invitrogen) in phosphate buffered saline (PBS) for 8 min, dissociated into a single cell suspension, and then fixed as described above. Stained cells were analyzed with a BD FACSAria II (BD Biosciences). Data retrieved from the sorting was analyzed with Flowjo software 9.3.3 (Tree Star, Ashland, OR).

Immunocytochemistry

All manipulations were performed at room temperature. Cultured primary and hiPSC-derived RPE cells were fixed with 4% paraformaldehyde in PBS for 20 min at room temperature. After washing with PBS, the cells were permeabilized with 0.2% Triton-X100 in PBS for 15 min and blocked with 2% bovine serum albumin in PBS for 30 min. Samples were incubated for 1 h with mouse anti-N-cadherin monoclonal antibody 1:1000 (GC-4, Sigma–Aldrich). The cells were washed with PBS and incubated with 1:1000 Alexa Fluor 488 F(ab')2 fragment of goat anti-mouse IgG 1:1000 (Molecular Probes) for 1 h. The samples were mounted with a Vectashield mounting medium containing DAPI (Vector Laboratories, Burlingame, CA). and examined with a Biozero-8000 fluorescence microscope (Keyence, Japan).

Supporting Information

Figure S1 Soft agar colony formation assay of hiPSCs, teratocarcinoma PA-1 cells and primary RPE cells. (A) hiPSCs (10000 cells, 6000cells and 3000 cells/well) were grown in soft agar for 10, 20 and 30 days with 10 μM Y-27632. (B) PA-1 cells (1000, 500, 300, 200, 100, 50, 30 cells/well) were grown in soft agar for 20 days. (C) Primary RPE cells (lot. A, 100,000, 60,000, 30,000 and 10,000 cells/well) were grown in soft agar for 30 days. (A–C) Cell growth was quantified using a CytoSelect kit and the results expressed as a relative fold change of the value of a blank well. Error bars represent the standard deviation of the measurements (n = 3).
(EPS)

Figure S2 Flow cytometry analysis of spiked hiPSCs cells in primary RPE. CFDA-stained hiPSCs (1%, 2,500 cells; 0.1%, 250 cells; 0.01%, 25 cells) were spiked into primary RPE (2.5×10^5 cells) and 1×10^5 cells were analyzed by flow cytometry. The numbers indicate the quantity of cells contained in the gate. (EPS)

Table S1 Probes and primers for qRT-PCR. (DOCX)

Acknowledgments

We would like to thank Masahiro Go, Hoshimi Kanemura and Akifumi Matsuyama for their valuable discussion on this paper. We also thank Satoshi Okamoto and Noriko Sakai for technical advice of RPE cell differentiation.

Author Contributions

Conceived and designed the experiments: TK SY YS. Performed the experiments: TK SY NH. Analyzed the data: TK SY S. Kusakawa NH YK KS MT SN S. Kawamata YS. Contributed reagents/materials/analysis tools: YK MT S. Kawamata. Wrote the paper: TK SY YS. Acquired the funding: SN S. Kawamata KS YS.

References

1. Thomson JA, Itskovitz-Eldor J, Shapiro SS, Waknitz MA, Swiergiel JJ, et al. (1998) Embryonic stem cell lines derived from human blastocysts. Science 282: 1145–1147.
2. Takahashi K, Tanabe K, Ohnuki M, Narita M, Ichisaka T, et al. (2007) Induction of pluripotent stem cells from adult human fibroblasts by defined factors. Cell 131: 861–872.
3. Kehat I, Kenyagin-Karsenti D, Snir M, Segev H, Amit M, et al. (2001) Human embryonic stem cells can differentiate into myocytes with structural and functional properties of cardiomyocytes. J Clin Invest 108: 407–414.
4. Zhang SC, Wernig M, Duncan ID, Brustle O, Thomson JA (2001) *In vitro* differentiation of transplantable neural precursors from human embryonic stem cells. Nat Biotechnol 19: 1129–1133.
5. Cai J, Zhao Y, Liu Y, Ye F, Song Z, et al. (2007) Directed differentiation of human embryonic stem cells into functional hepatic cells. Hepatology 45: 1229–1239.
6. Song Z, Cai J, Liu Y, Zhao D, Yong J, et al. (2009) Efficient generation of hepatocyte-like cells from human induced pluripotent stem cells. Cell Res 19: 1233–1242.
7. Osakada F, Jin ZB, Hirami Y, Ikeda H, Danjyo T, et al. (2009) *In vitro* differentiation of retinal cells from human pluripotent stem cells by small-molecule induction. J Cell Sci 122: 3169–3179.
8. Carr AJ, Vugler AA, Hikita ST, Lawrence JM, Gias C, et al. (2009) Protective effects of human iPS-derived retinal pigment epithelium cell transplantation in the retinal dystrophic rat. PLoS One 4: e8152.
9. Ben-David U, Benvenisty N (2011) The tumorigenicity of human embryonic and induced pluripotent stem cells. Nat Rev Cancer 11: 268–277.
10. Knoepfler PS (2009) Deconstructing stem cell tumorigenicity: a roadmap to safe regenerative medicine. Stem Cells 27: 1050–1056.
11. Hentze H, Soong PL, Wang ST, Phillips BW, Putti TC, et al. (2009) Teratoma formation by human embryonic stem cells: evaluation of essential parameters for future safety studies. Stem Cell Res 2: 198–210.
12. Lee AS, Tang C, Cao F, Xie X, van der Bogt K, et al. (2009) Effects of cell number on teratoma formation by human embryonic stem cells. Cell Cycle 8: 2608–2612.
13. Noaksson K, Zoric N, Zeng X, Rao MS, Hyllner J, et al. (2005) Monitoring differentiation of human embryonic stem cells using real-time PCR. Stem Cells 23: 1460–1467.
14. Pera MF, Reubinoff B, Trounson A (2000) Human embryonic stem cells. J Cell Sci 113(Pt 1): 5–10.
15. Draper JS, Pigott C, Thomson JA, Andrews PW (2002) Surface antigens of human embryonic stem cells: changes upon differentiation in culture. J Anat 200: 249–258.
16. Van Aken EH, De Wever O, Van Hoorde L, Bruyneel E, De Laey JJ, et al. (2003) Invasion of retinal pigment epithelial cells: N-cadherin, hepatocyte growth factor, and focal adhesion kinase. Invest Ophthalmol Vis Sci 44: 463–472.
17. Hamburger AW, Salmon SE (1977) Primary bioassay of human tumor stem cells. Science 197: 461–463.
18. Watanabe K, Ueno M, Kamiya D, Nishiyama A, Matsumura M, et al. (2007) A ROCK inhibitor permits survival of dissociated human embryonic stem cells. Nat Biotechnol 25: 681–686.
19. Ohgushi M, Matsumura M, Eiraku M, Murakami K, Aramaki T, et al. (2010) Molecular pathway and cell state responsible for dissociation-induced apoptosis in human pluripotent stem cells. Cell Stem Cell 7: 225–239.
20. Albini A, Iwamoto Y, Kleinman HK, Martin GR, Aaronson SA, et al. (1987) A rapid *in vitro* assay for quantitating the invasive potential of tumor cells. Cancer Res 47: 3239–3245.
21. Miller JNMJC (2005) Statistics and Chemometrics for Analytical Chemistry Fifth edition. Harlow: Person Education Limited.
22. Andrews PW, Banting G, Damjanov I, Arnaud D, Avner P (1984) Three monoclonal antibodies defining distinct differentiation antigens associated with different high molecular weight polypeptides on the surface of human embryonal carcinoma cells. Hybridoma 3: 347–361.
23. Nakagawa M, Koyanagi M, Tanabe K, Takahashi K, Ichisaka T, et al. (2008) Generation of induced pluripotent stem cells without Myc from mouse and human fibroblasts. Nat Biotechnol 26: 101–106.
24. Okita K, Hong H, Takahashi K, Yamanaka S (2010) Generation of mouse-induced pluripotent stem cells with plasmid vectors. Nat Protoc 5: 418–428.
25. Maekawa M, Yamaguchi K, Nakamura T, Shibukawa R, Kodanaka I, et al. (2011) Direct reprogramming of somatic cells is promoted by maternal transcription factor Glis1. Nature 474: 225–229.
26. Tang C, Lee AS, Volkmer JP, Sahoo D, Nag D, et al. (2011) An antibody against SSEA-5 glycan on human pluripotent stem cells enables removal of teratoma-forming cells. Nat Biotechnol 29: 829–834.
27. Levenbook IS, Petricciani JC, Qi Y, Elisberg BL, Rogers JL, et al. (1985) Tumorigenicity testing of primate cell lines in nude mice, muscle organ culture and for colony formation in soft agarose. J Biol Stand 13: 135–141.
28. Nam Y, Chen C, Gregory RI, Chou JJ, Sliz P (2011) Molecular Basis for Interaction of let-7 MicroRNAs with Lin28. Cell 147: 1080–1091.
29. West JA, Viswanathan SR, Yabuuchi A, Cunniff K, Takeuchi A, et al. (2009) A role for Lin28 in primordial germ-cell development and germ-cell malignancy. Nature 460: 909–913.

Journal of Pharmaceutical and Biomedical Analysis 70 (2012) 718–726

Contents lists available at SciVerse ScienceDirect

Journal of Pharmaceutical and Biomedical Analysis

journal homepage: www.elsevier.com/locate/jpba

Comparative studies on glycoproteins expressing polylactosamine-type N-glycans in cancer cells

Yosuke Mitsui [a], Keita Yamada [a], Sayaka Hara [a], Mitsuhiro Kinoshita [a], Takao Hayakawa [b], Kazuaki Kakehi [a,*]

[a] School of Pharmacy, Kinki University, Kowakae 3-4-1, Higashi-Osaka 577-8502, Japan
[b] Pharmaceutical Research and Technology Institute, Kinki University, Kowakae 3-4-1, Higashi-Osaka 577-8502, Japan

ARTICLE INFO

Article history:
Received 8 March 2012
Received in revised form 21 June 2012
Accepted 25 June 2012
Available online 4 July 2012

Keywords:
Cancer-specific glycoproteins
N-glycans
LC–MS
Lectin affinity chromatography
Western blot

ABSTRACT

In the series of our previous reports, we showed that some cancer cell lines specifically express polylactosamine-type N-glycans and such glycans were often modified with fucose and sulfate residues. To confirm the proteins expressing these glycans, glycopeptide mixture obtained by digestion of whole protein fractions with trypsin was captured by a polylactosamine-specific lectin, *Datura strasmonium* agglutinin (DSA). And the peptides and glycans of the captured glycopeptides after digestion with N-glycoamidase F were extensively analyzed by HPLC and MS techniques. We found that some glycoproteins such as CD107a and CD107b commonly contained polylactosamine-type glycans in all the examined cancer cells. But integrin-α5 (CD49e) and carcinoembryonic antigen-related cell adhesion molecule 5 (CD66e) having these glycans were specifically found in U937 (human T-lymphoma) and MKN45 (human gastric cancer) cells, respectively. These data clearly indicate that specific glycans attached to specific proteins will be promising markers for specific tumors with high accuracy.

1. Introduction

Glycans in glycoconjugates such as glycoproteins, proteoglycans and glycolipids participate in various biological events such as cell recognition, cell–cell interaction, inflammation, and disease progression [1,2]. Aberrant glycosylation has been known to be associated with various human diseases, particularly with tumors. And a number of clinical cancer biomarkers are often glycoproteins such as carcinoembryonic antigen (CEA; CD66) as a marker of colorectal cancer, cancer antigen 125 (CA-125) for diagnosis of ovarian cancer and prostate-specific antigen (PSA).

Biosynthesis of the glycans in glycoproteins is regulated by a number of factors such as (a) expression of related glycosyltransferases and/or glycosidases, (b) proper locations, and (c) the functional machinery of sugar nucleotides. Thus, micro environmental changes in the synthesis of glycans greatly affect their synthetic efficiency and also their structures. For example, complex-type N-glycans having polylactosamine-type structures are predominantly present when cells are tumorized. However, it has been challenging to analyze specific glycans in comprehensive and quantitative manner, because extremely a minute amount of glycans are available in biological samples.

In our previous papers, we proposed a series of methods for the analysis of glycans of glycoproteins in biological samples [3–5]. The methods include several separation/analysis steps. Initially, total glycan pool obtained from biological samples such as cell membrane fractions by enzymatic/chemical methods was fluorescently labeled with 2-aminobenzoic acid (2AA), and separated based on the number of sialic acid residues attached to the glycans using affinity chromatography on a serotonin-immobilized stationary phase. In this step, we can determine total amounts of glycans as well as those of each category of glycans (asialo/high-mannose, mono-, di-, tri- and tetra-sialoglycans). Then, the collected glycan groups were analyzed by LC/MS^n technique. Capillary affinity electrophoresis and digestion with specific exoglycosidases for linkage analysis were also employed. Based on the studies using these techniques, we found that U937 cells (histiocytic lymphoma cells), ACHN cells (human kidney glandular cancer cells), MKN45 cells (human gastric cancer cells), A549 cells (human lung cancer cells), and Jurkat cells (acute T-cell leukemia) express a large amount of N-glycans having polylactosamine residues.

There are a number of reports regarding the functions and distributions of polylactosamine-type glycans [6]. And the proteins to which polylactosamine-type glycans are attached were also reported by Fukuda et al. [7]. They employed *Datura stramonium* agglutinin (DSA) affinity chromatography for capturing proteins carrying polylactosamine-type glycans [8]. Togayachi et al. reported that polylactosamine residues on glycoproteins influenced basal levels of lymphocyte and macrophage activation.

* Corresponding author. Tel.: +81 6 6721 2332; fax: +81 6 6721 2353.
E-mail address: k_kakehi@phar.kindai.ac.jp (K. Kakehi).

0731-7085/$ – see front matter © 2012 Elsevier B.V. All rights reserved.
http://dx.doi.org/10.1016/j.jpba.2012.06.035

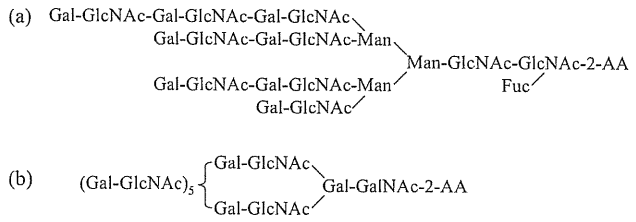

Fig. 1. Typical structures of polylactosamine-type glycans. (a) N-glycans and (b) O-glycans.

They employed *Lycopersicon esculentum* (tomato) agglutinin (LEA), which recognizes the repeats of polylactosamine units [9].

In our previous report on the analysis of N-glycans in cancer cells, we found that lactosamine units were elongated at all the branches of tri- and tetra-antennary glycans (Fig. 1a) [3]. In contrast, they form a long chain of polylactosamine-units in mucin-type O-glycans (Fig. 1b) [4].

This is probably due to branching effect of N-glycans which accerelate the addition of lactosamine residues to every branches of the glycans. We need to clarify the reasons why polylactosamine-glycans are elongated in different manners in Asn-linked N-glycans and mucin-type O-glycans in order to understand glycan profiles for clinical use.

In the present study, we attempted to confirm glycoprotein(s) which express polylactosamine-type N-glycans in several cancer cell lines. In addition, polylactosamine-carrying glycoproteins are compared among several cancer cell lines. And we propose that comparative studies of the proteins which express specific glycans on various cancer cell lines afford important information on diagnosis for cancer stages.

2. Materials and methods

2.1. Materials

Enzyme. Peptide N-glycoamidase F (EC 3.5.1.52) was obtained from Roche Diagnostics (Mannheim, Germany). Neuraminidase (*Arthrobacter ureafaciens*) was kindly donated by Dr. Ohta (Marukin-Bio, Uji, Kyoto, Japan). Benzonase was obtained from Novagen (Darmstadt, Germany). TPCK-treated trypsin was from Worthington (Lakewood, NJ). *Antibody*. LAMP-1 (H4B3) mouse IgG_1 monoclonal, LAMP-2 (H4B4) mouse IgG_1 monoclonal and integrin α5 (D-9) mouse IgG_{2a} monoclonal were from Santa Cruz Biotechnology (Santa Cruz, CA). Basigin (MEM-M6/1) mouse IgG_1 monoclonal was from Abcam (Cambridge, UK). Transferrin receptor mouse IgG_1 monoclonal was kindly donated by Dr. Yagi (Kinki University, School of Pharmacy). *Chemicals*. 2-Iodoacetamide was from Tokyo Kasei (Chuo-ku, Tokyo, Japan). Dithiothreitol (DTT) was obtained from Nacalai Tesque (Nakagyo-ku, Kyoto, Japan). 3,3′-Diaminobenzidine, tetrahydrochloride (DAB) was obtained from DOJINDO (Kamimashiki-gun, Kumamoto, Japan). 2-Aminobenzoic acid (2AA) and sodium cyanoborohydride for fluorescent labeling of oligosaccharides were from Tokyo Kasei. Coomassie brilliant blue G-250 was purchased from Bio-Rad (Hercules, CA). Sephadex LH-20 was from Amerscham Bioscience (Upsala, Sweden). Vivaspin 500 was obtained from Sartorius (Goettingen, Germany). DSA-agarose and DSA-biotin were obtained from Seikagaku Kogyo (Chuoku, Tokyo, Japan). LEA-agarose and VECTA Elite ABC mouse IgG kit for Western blotting were obtained from Vector Labs (Burlingame, CA). Immobilon-P Transfer Membrane (PVDF) was obtained from Millipore (Bedford, MA). Protein inhibitor cocktail for animal cells was obtained from Nacalai Tesque. Protein G Sepharose 4 Fast Flow was obtained from GE Healthcare (Upsala, Sweden). All other reagents and solvents were of the highest grade commercially available or of HPLC grade. All aqueous solutions were prepared using water purified with a Milli-Q purification system (Millipore, Bedford, MA).

2.2. Cell culture

In the present study, we used the following cell lines: U937 cells (human T-lymphoma cells), ACHN cells (human kidney glandular cancer cells), MKN45 cells (human gastric cancer cells), A549 cells (human lung cancer cells), and Jurkat cells (acute T cell leukemia). The cells except for A549 were cultured in RPMI-1640 medium supplemented with 10% (v/v) fetal calf serum and 1% (v/v) penicillin–streptomycin solution (10,000 U penicillin and 10 mg streptomycin/mL; Nacalai Tesque). A549 cells were cultured in Dulbecco's modified Eagle's medium supplemented with 10% (v/v) fetal calf serum and 1% (v/v) penicillin–streptomycin solution. Fetal calf serum was previously kept at 56 °C for 30 min. The cells were cultured at 37 °C under 5% CO_2 atmosphere, and harvested at 80% confluent state. Cells (1×10^7 cells) were washed with phosphate buffered saline (PBS), and collected by centrifugation at 1000 rpm for 20 min.

2.3. Extraction of whole proteins from cancer cells and digestion with trypsin

Cancer cells (1.0×10^7 cells) were suspended in PBS containing 1 mM EDTA (50 μL), and kept at room temperature for 15 min. Extraction reagent (7 M urea, 2 M thiourea, 4% CHAPS, 30 mM Tris–HCl (pH 8.5, 268 μL)), 1 M DTT (17 μL) and benzonase (125 units, 5 μL) were added to the suspended cells. After 30 min, the mixture was centrifuged at 8000 × *g* for 15 min. The supernatant layer was collected and boiled for 5 min at 100 °C, and evaporated to dryness by a centrifugal evaporator (Speed Vac, Servant, Sunnydale, CA). Guanidine solution (2 mM EDTA, 0.5 M Tris–HCl and 4 M guanidine (pH 8.5, 80 μL)) was added to the lyophilized material. After dissolution of the lyophilized material, 0.18 M DTT in guanidine solution (40 μL) was added to the mixture. The mixture was kept at 37 °C for 90 min. After addition of 0.18 M iodoacetamide in guanidine solution (155 μL), the mixture was kept for 45 min in a dark place. After addition of acetone solution (85% acetone, 5% triethylamine, 5% acetic acid in water (1.7 mL)), the mixture was kept at −20 °C for 30 min, and the precipitate was collected by centrifugation at 8000 × *g* for 15 min and washed with 75% ethanol (1 mL × 2). The precipitate was evaporated to dryness by a centrifugal evaporator. The dried material was digested with trypsin (100 μg) in 2 M urea, 0.1 M Tris–HCl (pH 8.6, 800 μL) at 37 °C overnight. After the reaction, the mixture was boiled for 10 min, and the supernatant was collected, and passed through an ultrafiltration membrane (MW cut off, 5000 Da). The residual solution on the membrane was used as a mixture of glycopeptides.

2.4. Collection of glycopeptides having polylactosamine-type glycans by lectin affinity chromatography using a DSA-immobilized agarose column, and digestion of the captured glycopeptides with N-glycoamidase F

The solution of the glycopeptide mixture obtained as described above was applied to a DSA-immobilized column (DSA 3.8 mg (7.9 nmol)/1 mL of agarose) which had been previously equilibrated with PBS. Unbound peptides were eluted with 15 mL of PBS. Then, bound glycopeptides were eluted with 0.1 M N-acetyl D-glucosamine in PBS (15 mL). The bound and unbound fractions were passed through an ultrafiltration membrane (MW cut off, 3000 Da), respectively, and the residual solution on the membrane was evaporated to dryness by a centrifugal evaporator. The dried materials were digested with N-glycoamidase F (2 units, 2 μL) in

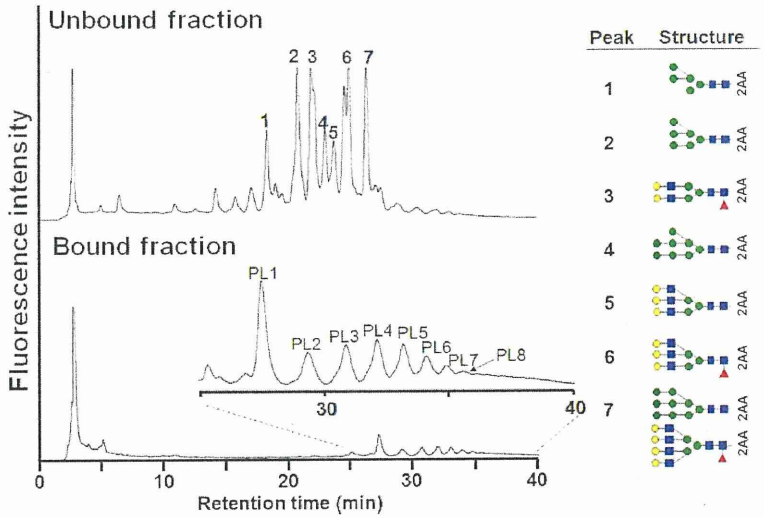

Fig. 2. HPLC analysis of the peaks observed in DSA-bound fractions. The N-glycans were previously digested with neuraminidase. Analytical conditions: column, TSK-Gel Amide-80 (4.6 mm × 250 mm); eluent: A, 0.2% acetic acid/acetonitrile; B, 0.5% acetic acid–0.3% triethylamine/water. Gradient elution, 0–2 min (30% solvent B), 2–82 min (30–95% solvent B), 82–102 min (95% solvent B). Detection, Ex 350 nm, Em 425 nm. Column temp. 40 °C.

100 mM phosphate buffer (pH 7.5, 100 μL) at 37 °C overnight. After keeping the enzyme reaction mixture in the boiling water bath for 10 min, the mixture was centrifuged at 8000 × *g* for 10 min. The supernatant solutions were collected and lyophilized to dryness.

2.5. *Fluorescent labeling of the released N-glycans with 2-aminobenzoic acid (2AA) and analysis of the labeled glycans by HPLC*

A portion (1.2×10^7 cells) of the dried material obtained by digestion with N-glycoamidase F (see Section 2.4) was dissolved in 2AA solution (100 μL) which was freshly prepared by dissolution of 2AA (30 mg) and sodium cyanoborohydride (30 mg) in methanol (1 mL) containing 4% sodium acetate and 2% boric acid. The mixture was kept at 80 °C for 1 h. After cooling, water (100 μL) was added to the mixture, and applied to a column of Sephadex LH-20 (1.0 cm i.d., 30 cm length) equilibrated with 50% aqueous methanol. Fluorescent intensities of each fraction were monitored at 410 nm irradiated with a 335-nm light. The earlier eluted fluorescent fractions were pooled and evaporated to dryness under reduced pressure. The lyophilized materials were digested with neuraminidase (2 munits, 4 μL) in 20 mM acetate buffer (pH 5.0, 100 μL) at 37 °C overnight. After keeping the mixture in the boiling water bath for 10 min, the mixture was centrifuged at 8000 × *g* for 10 min. The supernatant solution was collected and lyophilized to dryness, and the dried materials were dissolved in water. And a portion (5×10^6 cells; 3 μL) was analyzed by a Jasco HPLC apparatus equipped with two PU-980 pumps and a Jasco FP-920 fluorescence detector (Hachio-ji, Tokyo, Japan). Separation was done with an Amide-80 column (Tosoh, 4.6 × 250 mm) using a linear gradient formed by 0.2% acetic acid in acetonitrile (solvent A) and 0.5% acetic acid in water containing 0.3% triethylamine (solvent B). The column was initially equilibrated and eluted with 70% solvent A for 2 min, from which point solvent B was increased to 95% over 80 min, and kept at this composition for further 100 min. Flow rate was kept at 1.0 mL/min. The observed peaks were collected and lyophilized to dryness for the analysis by matrix-assisted laser-desorption ionization time-of-flight (MALDI-TOF) mass spectrometry.

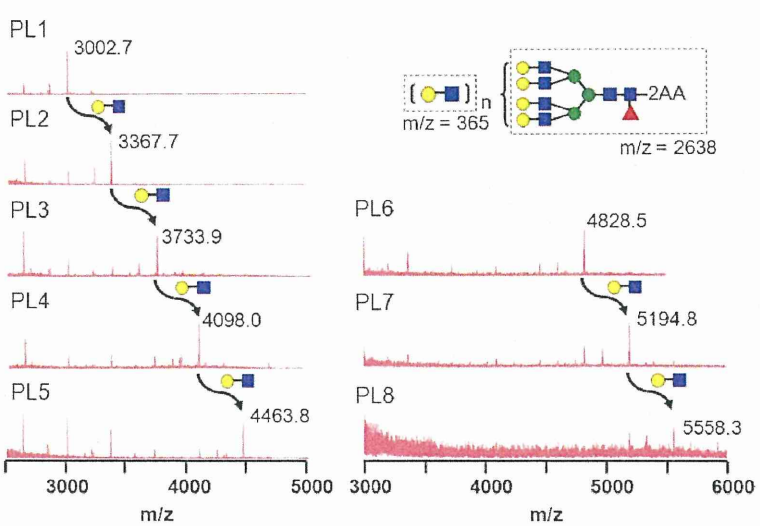

Fig. 3. MS analysis of the peaks observed in Fig. 2.

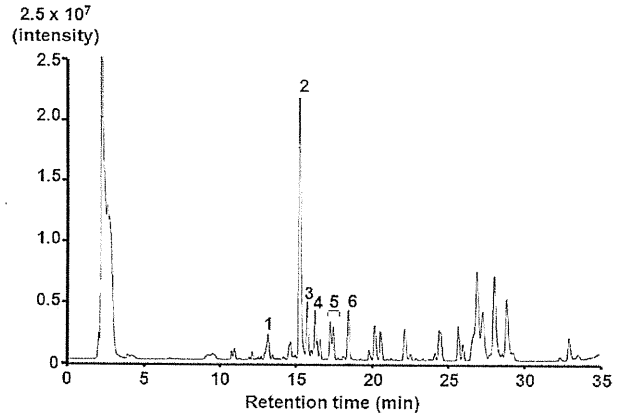

Fig. 4. Total ion chromatogram of DSA-bound glycopeptides. Analytical conditions: see Section 2.

2.6. MALDI-TOF MS analysis

MALDI-TOF MS spectra of 2AA-labeled glycans were acquired on a MALDI-QIT TOF mass spectrometer (AXIMA-QIT, Shimadzu, Kyoto, Japan). Acquisition and data processing were controlled by a Launchpad software (Kratos Analytical, Manchester, UK). Typically, a 0.5-μL portion of the matrix solution (DHB; 10 mg/mL in 30% ethanol/0.1% trifluoroacetic acid) was deposited on the stainless steel target plate and allowed to dry. Then, a portion (0.5 μL) of the appropriately diluted analyte solution (typically ca. 1 pmol/μL) was used to cover the matrix on the target plate and allowed to dry at room temperature.

2.7. Liquid chromatography (LC) ion-trap time-of-flight (IT-TOF) MS analysis of peptides

Positive electrospray ionization (ESI)-MS analyses were conducted with an LC–IT-TOF MS instrument (Shimadzu, Kyoto) connected with an HPLC system (LC-20AD pump, CTO-20AC column oven, and CBM-20A system controller; Shimadzu, Kyoto). A portion (5×10^6 cells; 3 μL) of the aqueous solution of the peptide mixture obtained after digestion with N-glycoamidase F (see Section 2.4) was injected to a reverse-phase column (HiQ sil C_{18V} column, 2.1 mm × 150 mm; KYA TECH), and analyzed using the following gradient program. Solvent A was 5% acetonitrile/0.1% formic acid. Solvent B was 95% acetonitrile/0.1% formic acid. The column was initially equilibrated and eluted with 95% solvent A for 5 min, from which point solvent B was increased to 75% over 30 min at a flow rate of 0.2 mL/min. Column temperature was kept at 40 °C. The MS apparatus was operated at a probe voltage of 4.50 kV, CDL temperature of 200 °C, block heater temperature of 200 °C, nebulizer gas flow of 1.5 L/min, ion accumulation time of 30 ms. MS range was from *m/z* 200 to 2000, and MS/MS range also from *m/z* 200 to 2000. CID parameters were as follows: energy, 50%; collision gas, 50%. Monoisotopic ion was used as the precursor ion. MS data were processed with LCMS solution ver. 3.6 software (Shimadzu).

2.8. Peptides mass finger printing

For protein identification, Mascot generic format (MGF) files generated from MS/MS spectra were uploaded to MASCOT search (Matrix Science, London, UK: http://www.matrixscience.com). The parameters for database search were as follows: protein database was set to Swiss PROT. Taxonomy was set to homo sapience. One trypsin missed cleavage was allowed. The mass tolerance was set to 0.5 Da for precursor ions and 0.6 Da for product ions. Carbamidomethyl (C) was chosen as a fixed modification. Deamidation (NQ) was chosen for variable modifications. Data format was chosen as Mascot generic, and instrument was chosen as ESI-TRAP-TOF.

2.9. Sodium dodecyl sulfate-polyacrylamide gel electrophoresis (SDS-PAGE)

After addition of SDS-PAGE sample buffer (250 mM Tris–HCl (pH 6.8)–4.6% SDS, 20% glycerol), 2-mercaptoethanol and water (10:9:1, 2 mL) to the cell pellet (2×10^7 cell), the mixture was vortexed, and boiled for 10 min. The supernatant was collected after centrifugation and used for SDS-PAGE. SDS-PAGE was performed with a Mini protean 3 Cell and a POWER PAC 3000 (Bio-Rad, Hercules, CA). The amount of the applied protein was 25 μg/lane. Separation gel was 10%. Electrophoresis buffer was 25 mM Tris, 198 mM glycine, 1% (w/v) SDS in water.

After SDS-PAGE, the gel was stained with Coomassie brilliant blue G-250 (CBB) for 1 h. CBB solution contains 40% methanol, 10% acetic acid, and 0.2% Coomassie brilliant blue G-250. The gel was destained with 40% methanol–10% acetic acid.

2.10. Western blot

Western blot was performed with a semi-dry electrophoretic transfer cell (Trans-Blot SD, Bio-Rad, Hercules, CA). PVDF membrane was kept in methanol for 1 min and in the blotting buffer (48 mM Tris, 39 mM glycine and 20% methanol (pH9.0)) for 1 h. Cell lysate (25 μg as protein) of U937 cells was resolved using reducing 9% SDS-PAGE and transferred to a PVDF membrane. The membrane was incubated in blocking buffer (5% skim milk, 0.05% Tween 20 in PBS). After washing with 0.05% Tween 20/PBS (20 mL 4×), the membrane was reacted with primary antibody overnight. All the primary antibodies were used at the same concentration (5 μg/mL, 5 mL). After washing with 0.05% Tween 20/PBS (20 mL 4×), the membrane was reacted with biotin conjugated with secondary antibodies (5 μg/mL, 5 mL) for 1 h. After washing with 0.05% Tween 20/PBS (20 mL), the PVDF membrane was reacted with HRP labeled avidin (5 μg/mL, 5 mL in PBS) for 1 h. After washing with 0.05% Tween 20/PBS (20 mL 4×), the membrane was visualized with 0.05% DAB, 0.0031% hydrogen peroxide in 100 mM Tris–HCl buffer (pH 7.5).

2.11. Lectin blot

SDS-PAGE and electrophoretic transferring were performed in the same manner as described above. After the gel was transferred to a PVDF membrane, the membrane was incubated in 0.05% Tween 20 in PBS, and reacted with biotin-labeled DSA lectin (5 μg/mL, 5 mL) for 1 h. After washing the membrane with 0.05% Tween 20 in PBS (20 mL 4×), the membrane was reacted with HRP-labeled avidin (5 μg/mL, 5 mL) for 30 min. After washing with 0.05% Tween 20 in PBS (20 mL 4×), the membrane was visualized with 0.05% DAB, 0.0031% hydrogen peroxide in 100 mM Tris–HCl buffer (pH 7.5).

2.12. Immunoprecipitation of target proteins

Lysis buffer (20 mM HEPES, 150 mM NaCl, 1 mM EDTA, 1.0% Triton X-100, 0.5% deoxycholate, 0.1% SDS, 950 μL) and protease inhibitor (50 μL) were added to the pellet of U937 cells (2×10^7 cells). The mixture was vortexed for 10 min and incubated on an ice bath for 30 min, and centrifuged at 8000 × *g* for 30 min. The supernatant was collected, and used for immunoprecipitation.

Antibody for the specific protein (50 μg/mL, 100 μL) was added to Protein G Sepharose (100 μL), and the mixture was incubated for

Table 1
Glycoproteins identified in whole proteins of U937.

Peak no.	Proposed proteins	Peptide sequence	Precursor mass (*m/z*)	Score	Subcellular location
1	Integrin α5 (CD49e)	NL***NNS***QSDVVSFR	$[M+2H]^{2+}$ = 741.32	31	Membrane
2	Basigin (CD147)	ILLTCSL***NDS***ATEVTGHR	$[M+3H]^{3+}$ = 663.32	42	cell membrane, melanosome
3	Lysosome-associated membrane glycoprotein-1 (CD107a)	SSCGKE***NTS***DPSLVIAFGR	$[M+3H]^{3+}$ = 675.97	13	Cell membrane, endosome membrane, lysosome membrane
4	4F2 cell-surface antigen heavy chain (CD98)	SLVTQYL***NAT***GNR	$[M+2H]^{2+}$ = 719.35	69	Apical cell membrane, melanosome
	Sortilin	DITDLI***NNT***FIR	$[M+2H]^{2+}$ = 718.37	25	Cell membrane
5	Lysosome-associated membrane glycoprotein-1 (CD107a)	SGPK***NMT***FDLPSDATVVL***NR***	$[M+3H]^{3+}$ = 722.01	23	Cell membrane, endosome membrane, lysosome membrane
	Lysosome-associated membrane glycoprotein-2 (CD107b)	VASVININP***NTT***HSTGSCR	$[M+3H]^{3+}$ = 676.99	21	Cell membrane, endosome membrane, lysosome membrane
6	Transferrin receptor protein-1 (CD71)	DFEDLYTPV***NGS***IVIVR	$[M+2H]^{2+}$ = 969.47	12	Cell membrane, melanosome

1 h. Protein G Sepharose thus prepared was washed with PBS (1 mL 3×), and the protein mixture obtained from the cells (1×10^7 cells, see above) was added. The mixture was incubated at 4 °C overnight with gentle shaking. Protein G Sepharose was washed with PBS (1 mL 6×). After addition of SDS sample buffer (20 μL) and 2-mercaptoethanol (2 μL), Protein G Sepharose was boiled for 10 min. The supernatant was collected by centrifugation, and used for SDS-PAGE analysis.

2.13. In-gel digestion with N-glycoamidase F

Specific proteins collected by immunoprecipitation were analyzed by SDS-PAGE followed by staining with CBB. After changing the destaining solution with water, bands of specific proteins detected by Western blot were cut, and the gel pieces were destained with 30% acetonitrile (300 μL 2×) for 30 min and dehydrated with acetonitrile (200 μL 2×) for 10 min. After drying the gel pieces, the gel pieces were digested with N-glycoamidase F (2 units, 2 μL) in 100 mM phosphate buffer (pH 7.5, 100 μL) at 37 °C overnight. N-Glycans thus released were extracted with water (200 μL 3×) for 30 min, and the supernatant solution was lyophilized to dryness for labeling with 2AA.

3. Results and discussion

3.1. Identification of glycoproteins carrying polylactosamine-type N-glycans in U937 cells

Our group previously reported that U937 cells (histiocytic lymphoma cells) specifically expressed large amount of polylactosamine-type N-glycans [3]. As the initial study, we identified glycoproteins carrying polylactosamine-type N-glycans in U937 cells.

After whole proteins collected from U937 cells were digested with trypsin, DSA-immobilized and LEA-immobilized agarose columns were used for capturing polylactosamine-carrying peptides. The collected bound fractions from each of DSA and LEA immobilized columns were digested with N-glycoamidase F, and the released N-glycans were labeled with a fluorescent reagent, 2AA. Then, the mixture of the fluorescent labeled glycans were digested with neuraminidase, and analyzed by HPLC and MALDI-TOF MS. In the previous studies on the comprehensive analyses of N-glycans in various cancer cells, we found that lactosamine residues are attached to all the branches of tetraantennary glycans as shown in Fig. 1a [3]. DSA lectin preferentially recognizes tri- and tetra-antennary glycans [10]. On the other hand, LEA lectin binds to an elongated polylactosamine chain in glycans as indicated in Fig. 1b [9]. As shown in Fig. 2, characteristic ladder peaks (PL1–PL8) due to polylactosamine-type glycans were observed in DSA-bound fractions. In contrast, high-mannose, tri- and tetra-antennary glycans were observed abundantly in unbound fractions (the list of the structures in Fig. 2).

However, glycan peaks were not observed in LEA-bound fractions (data not shown). This means that lactosamine units are bound to the branches of tetraantennary glycans as indicated in Fig. 1a. The mass spectra of the peaks observed in the bound fractions are shown in Fig. 3.

The molecular ion at *m/z* 3002 (PL1) corresponds to the monofucosylated tetra-antennary glycan to which one lactosamine residue is attached. And the molecular ions increase by *m/z* 365 from PL1 to PL8. PL8 showing the largest molecular ion at *m/z* 5558 is the tetra-antennary glycan having eight polylactosamine residues. We already reported the structure of PL4 as shown in Fig. 1a [3]. From these results, polylactosamine-type glycans were selectively concentrated in the DSA-bound glycopeptides. It should be noticed that other glycans such as those having high-mannose type glycans were not included in the bound fractions. And this means that polylactosamine-type N-glycans preferentially attach to the specific peptide (see below).

Based on the analyses of the N-glycans, peptide portions of the DSA-bound glycopeptides which contained polylactosamine-type glycans were analyzed by LC–MS (Fig. 4).

More than 25 peaks were observed in the total ion chromatogram. The peaks observed from 13 min to 19 min showed higher molecular ions than *m/z* 1000. On the other hand, the peaks eluted later than 20 min showed low molecular ions (less than *m/z* 500). The small peptides of which molecular weights are less than *m/z* 500 have little information on amino acid sequences. Therefore, we analyzed the peaks showing large molecular ions by MS/MS, and identified that seven peaks were due to specific glycoproteins as shown in Table 1 by Mascot analysis.

Of the confirmed glycoproteins, integrin expressing multiantennary glycans was reported to play some functions on metastasis of tumors [11]. Lysosome-associated membrane glycoproteins (LAMP-1 and LAMP-2; peak 3 and peak 5) and basigin (peak 2) are glycoproteins having polylactosamine-type N-glycans [7,12,13]. CD98, transferrin receptor protein-1 as well as sortilin have N-glycans, although the presence of polylactosamine-type glycans was not clear [14–17].

Although glycoproteins in Table 1 possibly have the sequence to which polylactosamine-type glycans are attached, our method can not conclude this point. Therefore, glycoproteins that were assumed to be associated with the expression of polylactosamine-type glycans were identified by Western blot analysis (Fig. 5).

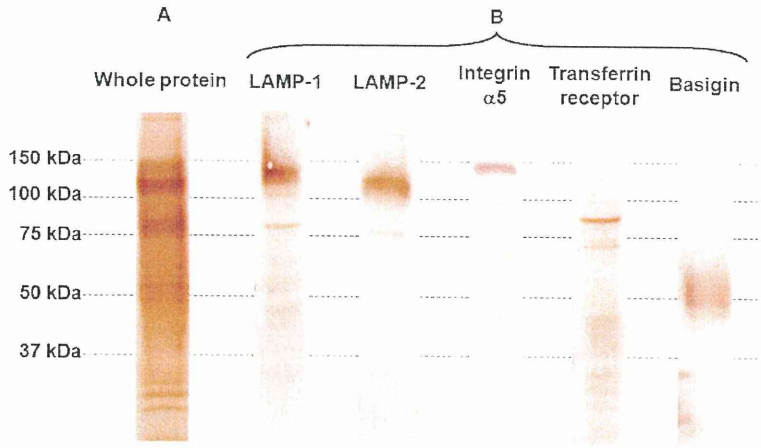

Fig. 5. Western blot and DSA lectin blot analysis of glycoproteins confirmed by shotgun analysis. (A) DSA lectin blot. (B) Western blot analysis of glycoproteins. Analytical conditions: separation gel, 10% T/2.6% C; blotting buffer: 48 mM Tris–39 mM glycine–20% methanol; blocking buffer for lectin blot, 0.05% Tween 20 in PBS; blocking buffer for Western blot, 5% skim milk–0.05% Tween 20 in PBS. Detection: HRP-DAB.

Whole protein fractions show the presence of a number of bands by DSA-lectin blot analysis (Fig. 5, lane A). The proteins identified by MASCOT analysis were confirmed by Western blot analysis (Fig. 5B). LAMP-1, LAMP-2 and integrin α5 could be clearly detected at around 100–150 kDa. Transferrin receptor protein-1 and basigin were also observed at ca. 80 kDa and 50–70 kDa, respectively. However, CD98, of which presence had been reported, was not detected (data not shown)[18]. These data are well consistent with those reported previously [13,19,20]. To verify the presence of polylactosamine-type N-glycans in these glycoproteins, we analyzed the glycans of the bands stained by Western blot analysis.

3.2. N-Glycan analysis of LAMP-1 and LAMP-2 obtained from U-937 cells by immunoprecipitation method

LAMP-1 and LAMP-2 purified by immunoprecipitation method were further separated by SDS-PAGE. And the bands at 100–150 kDa (see Fig. 5) were cut, and in-gel digested with N-glycoamidase F followed by labeling with 2AA. After neuraminidase digestion, N-glycans from LAMP-1 and LAMP-2 were analyzed by HPLC and MALDI-TOF MS. The results are shown in Fig. 6 and Table 2.

LAMP-1 and LAMP-2 contained high-mannose and complex type N-glycans abundantly. In addition, characteristic ladder peaks due to polylactosamine-type N-glycans were observed (Fig. 6). These peaks were confirmed by MALDI-TOF MS after collection of the peaks (Table 2). Fukuda's group reported the following results: LAMP-1 and LAMP-2 in colon carcinoma and human promyelocytic leukemia cells expressed tri- and tetra-antennary glycans as well as high-mannose type glycans. In addition, tetraantennary glycans having five or six lactosamine units were present abundantly in LAMP-1 and LAMP-2 molecules [8,21]. Our data clearly showed that LAMP-1 and LAMP-2 from U937 cells contained tetra-antennary glycans having elongated lactosamines (4 or 5 lactosamine units). It should be noticed that LAMP-1 contains larger polylactosamine-type N-glycans. Conventionally, the spots having polylactosamine glycans on 2D-gel were confirmed by lectin-blotting method. And the identified spots were analyzed by MS technique. Unfortunately, these techniques could not afford detailed information on glycan profiles. The proposed method in the present study focuses on specific glycopeptides having specific glycans, and will afford precise information on the changes of glycan profiles on specific glycoproteins with onset of diseases.

3.3. Comparative studies on the polylactosamine-carrying proteins present on some cancer cell lines

We compared proteins expressing polylactosamine-type glycans among various cancer cells using the methods employed for the analysis of U937 cells. Fig. 7 shows the results on the analyses of N-glycans of DSA-bound glycopeptides in A549 (human lung cancer cells), ACHN (human kidney glandular cancer cells), Jurkat (acute T cell leukemia) and MKN45 (human gastric adenocarcinoma) cells.

Characteristic ladder peaks indicate that these cell lines commonly express polylactosamine-type N-glycans. The ladder peaks observed in MKN45 cells are somewhat collapsed. This is because polylactosamine-type glycans are further modified with multiple fucose residues [3].

Based on these results, DSA-bound glycopeptides obtained from each cell line were digested with N-glycoamidase F, and the peptides having Asn-X-Ser/Thr sequences were analyzed by MS/MS analysis (Table 3). From five cancer cell lines, 25 glycoproteins in total were identified. Of the determined glycoproteins, 13 glycoproteins are CD antigens which express their own functions on the cell surface. CD98, LAMP-1 and basigin were commonly observed in all cell lines.

The sequence of SLVTQYL***NAT***GNR in CD98 was confirmed in all the examined cancer cell lines. In addition, the sequence, ***NMT***FDLPSDATVVL***NR*** (SGPK***NMT***FDLPSDATVVL***NR***) in LAMP1, was observed in four of five cancer cell lines, but the sequence was not detected in ACHN cells. The sequence, ILLTCSL***NDS***ATEVTGHR in basigin, was identified as the attaching site of polylactosamine-type glycans. These data indicate that polylactosamine-type N-glycans were abundantly observed in specific sequences. CD98, LAMP-1 and basigin were reported to be present in many cancer cells [22–24]. Especially, polylactosamine-type glycans of LAMP-1 and basigin play important roles in invasion/metastasis of cancer cells [12,21]. In addition, sialyl LewisX epitope (NeuAcα2–3Galβ1–4(Fucα1–3)GlcNACβ1–3Gal) expresses on polylactosamine-type glycans of LAMP-1 [25]. Basigin plays significant roles in tumors as well as other diseases by inducing production of matrix metalloproteinases by forming polymeric structures [13]. CD98 is observed abundantly in human tumor tissues such as melanoma, laryngeal carcinoma, lung adenocarcinoma, breast cancer, and renal cell cancers [26–29]. Functions on CD98 in relation to transport of amino acids, cell adhesion and malignant of cancer have been reported [17,29], but expression of polylactosamine-type N-glycans on CD98 is not known. The present

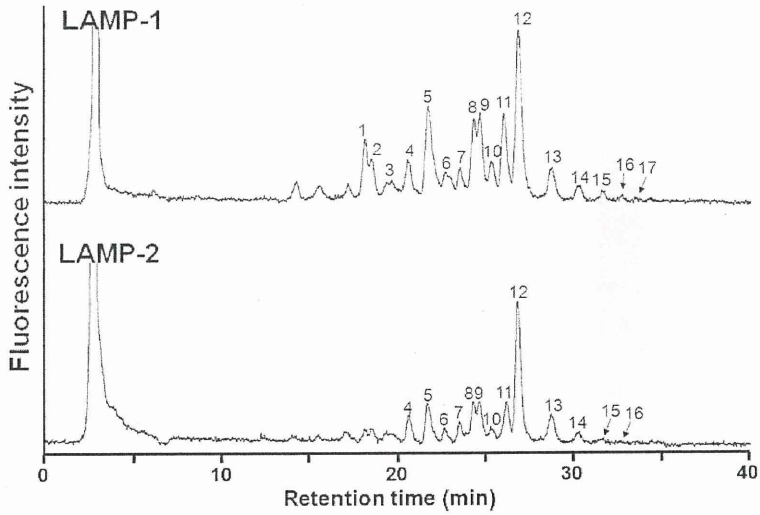

Fig. 6. HPLC analysis of N-glycans of immunoprecipitates of LAMP-1 and LAMP-2. Analytical conditions are also the same as those described in Fig. 1.

Table 2
List of oligosaccharides observed in LAMP-1 and LAMP-2.

Peak no.	Observed molecular mass		Calculated molecular mass	Monosaccharide composition
	LAMP-1	LAMP-2		
1	1356.7	1355.5		$Man_5GlcNAc_2$-2AA
2	1541.7	1542.6		$Man_3GalFucGlcNAc_3$-2AA
3	1746.9	1745.7		$Man_3GalFucGlcNAc_4$-2AA
4	1760.8	1761.0	1761.7	$Man_3Gal_2GlcNAc_4$-2AA
5	1906.9	1908.1	1907.7	$Man_3Gal_2FucGlcNAc_4$-2AA
6	1678.6	1678.9	1679.6	$Man_7GlcNAc_2$-2AA
	2110.8	2110.1	2110.8	$Man_3Gal_2FucGlcNAc_5$-2AA
7	2128.1	2126.1	2126.8	$Man_3Gal_3GlcNAc_5$-2AA
8	2271.7	2272.2	2272.8	$Man_3Gal_3FucGlcNAc_5$-2AA
9	1843.0	1840.9	1841.7	$Man_8GlcNAc_2$-2AA
	2271.7	2272.9	2272.8	$Man_3Gal_3FucGlcNAc_5$-2AA
10	2476.2	2476.0	2475.9	$Man_3Gal_3FucGlcNAc_6$-2AA
11	2002.5	2003.0	2003.7	$Man_9GlcNAc_2$-2AA
	2492.7	2492.0	2491.9	$Man_3Gal_4GlcNAc_6$-2AA
12	2637.6	2638.5	2638.0	$Man_3Gal_4FucGlcNAc_6$-2AA
13	3003.8	3003.6	3003.1	$Man_3Gal_5FucGlcNAc_7$-2AA
14	3367.8	3368.4	3368.2	$Man_3Gal_6FucGlcNAc_8$-2AA
15	3733.2	3733	43733.4	$Man_3Gal_7FucGlcNAc_9$-2AA
16	4098.3	4098	4098.5	$Man_3Gal_8FucGlcNAc_{10}$-2AA
17	4462.8		4463.6	$Man_3Gal_9FucGlcNAc_{11}$-2AA

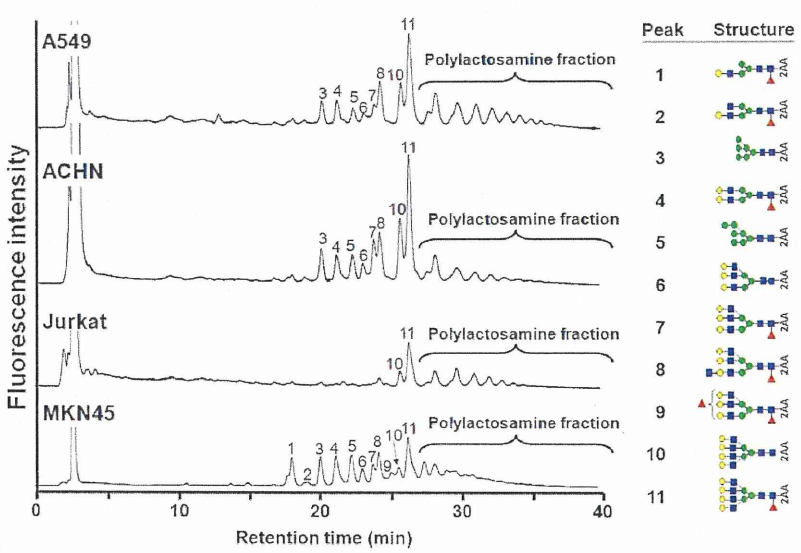

Fig. 7. HPLC analysis of N-glycans of DSA-bound glycopeptides from cancer cell.

Table 3
Comparison of possible polylactosamine-carrier proteins identified in whole protein of cancer cells.

Protein name	Jurkat	U937	MKN45	ACHN	A549
Receptor-type tyrosine-protein phosphatase C (CD45)					
YANITVDYLYNK (position: 230–241)	●				
NIETFTCDTQNITYR (position: 325–339)	●				
Integrin alpha-5 (CD49e)					
NLNNSQSDVVSFR (position: 771–783)		●			
CD59 glycoprotein					
TAVNCSSDFDACLITK (position: 40–55)	●			●	
CD63 antigen					
CCGAANYTDWEK (position: 145–156)				●	●
NRVPDSCCINVTVGCGINFNEK (position: 163–184)					●
Carcinoembryonic antigen-related cell adhesion molecule 5 (CD66e)					
EIIYPNASLLIQNIIQNDTGFYTLHVIK (position: 99–126)			●		
TLTLFNVTRNDTASYK (position: 199–214)			●		
Carcinoembryonic antigen-related cell adhesion molecule 6 (CD66c)					
ETIYPNASLLIQNVTQNDTGFYTLQVIK (position: 99–126)			●		
Transferrin receptor protein-1 (CD71)					
DFEDLYTPVNGSIVIVR (position: 242–258)		●			
4F2 cell-surface antigen heavy chain (CD98)					
DASSFLAEWQNITK (position: 355–368)	●			●	●
LLIAGTNSSDLQQILSLLESNK (position: 375–396)	●				
SLVTQYLNATGNR (position: 417–429)	●	●	●	●	●
Lysosome-associated membrane glycoprotein-1 (CD107a)					
SGPKNMTFDLPSDATVVLNR (position: 58–77)	●	●	●	●	
SSCGKENTSDPSLVIAFGR (position: 78–96)	●	●		●	
YSVQLMSFVYNLSDTHLFPNASSK (position: 111–134)			●		●
Lysosome-associated membrane glycoprotein-2 (CD107b)					
TVTISDHGTVTYNGSICGDDQNGPK (position: 63–87)	●				
VASVININPNTTHSTGSCR (position: 248–266)	●	●			
CD109 antigen					
TQDEILFSNSTR (position: 110–121)				●	
Basigin (CD147)					
ILLTCSLNDSATEVTGHR (position: 153–170)	●	●	●		●
Cation-dependent mannose-6-phosphate receptor					
LNETHIFNGSNWIMLIYK (position: 106–123)	●			●	●
Chondroitin sulfate proteoglycan 4					
GVNASAVVNVTVR (position: 2032–2044)					●
Fibronectin					
DQCIVDDITYNVNDTFHK (position: 516–533)				●	
Galectin-3-binding protein					
ALGFENATQALGR (position: 64–76)			●		
Neuroplastin					
ENGMPMDIVNTSGR (position: 275–288)					●
P2Y purinoceptor 12					
QAVDNLTSAPGNTSLCTRDYK (position: 2–22)				●	
Proactivator polypeptide					
TCDWLPKPNMSASCK (position: 93–107)					●
Solute carrier family 2, facilitated glucose transporter member 1					
VIEEFYNQTWVHR (position: 39–51)				●	
Solute carrier family 43 member 3					
DLCGPDAGPIGNATGQADCK (position: 45–64)	●				
Sortilin					
DITDLINNTFIR (position: 156–167)		●			
Synaptophysin-like protein 1					
GQTEIQVNCPPAVTENK (position: 56–72)	●				
Tetraspanin-13					
SVNPNDTCLASCVK (position: 133–146)	●				

data indicate that the common glycoproteins observed in cancer cell lines will be important markers, if N-glycans are also analyzed simultaneously.

Receptor-type tyrosine-protein phosphatase C (CD45) identified in Jurkat cells, carcinoembryonic antigen-related cell adhesion molecule 5 (CEA) in MKN45 cells, and CD63 antigens in ACHN and A549 cells are cell specific glycoproteins expressing polylactosamine-type glycans (Table 3). CD45 expresses commonly on T cells, and the attached polylactosamine-type glycans are ligands for galectin-1 [30]. CEA is observed abundantly in MKN45 cells, and closely related with cell–cell interactions through galectin-1 [31]. CEA also contains sialyl LewisX antigen [32]. Therefore, CEA molecules observed in MKN45 cells may contain Lewis antigens on their polylactosamine glycans. CD63 is observed abundantly as a specific antigen for melanoma, and contains large amount of polylactosamine-type glycans [33]. In addition, close relationship between CD63 and metastasis in lung and renal tumors has been reported [34].

The hitherto reported results described above indicate that polylactosamine-type glycans are observed in two types of glycoproteins: common glycoproteins on cancer cells and specific glycoproteins on a specific cancer cell line. Although we do not have the data on N-glycans on normal cells, the data obtained in the present study show significance of comparative studies on N-glycans among various cancer cells.

A number of proteins carrying polylactosamine-type glycans with relation to their biological functions on cancer cells have been reported. However, the studies were performed independently for each cell line, and there has been a big barrier to understand the roles of such glycan-carrying proteins as markers. As indicated in

this report, comprehensive studies using many cells at the same time will easily and clearly reveal the importance of these proteins.

4. Conclusion

In the series of studies on comprehensive analysis of glycans in cancer cells, we found that some specific glycans such as polylactosamine-type glycans are specifically and abundantly present in some cancer cells. In the present study, we proposed methods to determine specific proteins which carry specific glycans. The method is based on the following concepts: (1) finding of specific glycans expressing on specific tumors, (2) finding of specific proteins carrying these specific glycans, and (3) determination of the sequence to which specific glycans are attached.

The proposed method is well suited for the studies on these objectives, and will be a useful tool for finding glycan-based disease markers. Another project on O-glycan analysis affords complementary information on polylactosamine-type glycans in various cancer cells. Further studies on the relationship between proteins carrying polylactosamine-type N-glycans and O-glycans will lead to comprehensive and precise understanding of tumors.

References

[1] P.M. Drake, W. Cho, B. Li, A. Prakobphol, E. Johansen, N.L. Anderson, F.E. Regnier, B.W. Gibson, S.J. Fisher, Sweetening the pot: adding glycosylation to the biomarker discovery equation, Clin. Chem. 56 (2010) 223–236.

[2] M.M. Fuster, J.D. Esko, The sweet and sour of cancer: glycans as novel therapeutic targets, Nat. Rev. Cancer 5 (2005) 526–542.

[3] R. Naka, S. Kamoda, A. Ishizuka, M. Kinoshita, K. Kakehi, Analysis of total N-glycans in cell membrane fractions of cancer cells using a combination of serotonin affinity chromatography and normal phase chromatography, J. Proteome Res. 5 (2006) 88–97.

[4] K. Yamada, M. Kinoshita, T. Hayakawa, S. Nakaya, K. Kakehi, Comparative studies on the structural features of O-glycans between leukemia and epithelial cell lines, J. Proteome Res. 8 (2009) 521–537.

[5] K. Nakajima, Y. Oda, M. Kinoshita, K. Kakehi, Capillary affinity electrophoresis for the screening of post-translational modification of proteins with carbohydrates, J. Proteome Res. 2 (2003) 81–88.

[6] M. Fukuda, Cell surface glycoconjugates as onco-differentiation markers in hematopoietic cells, Biochim. Biophys. Acta 780 (1985) 119–150.

[7] S.R. Carlsson, M. Fukuda, The polylactosaminoglycans of human lysosomal membrane glycoproteins lamp-1 and lamp-2. Localization on the peptide backbones, J. Biol. Chem. 265 (1990) 20488–20495.

[8] N. Lee, W.C. Wang, M. Fukuda, Granulocytic differentiation of HL-60 cells is associated with increase of poly-N-acetyllactosamine in Asn-linked oligosaccharides attached to human lysosomal membrane glycoproteins, J. Biol. Chem. 265 (1990) 20476–20487.

[9] A. Togayachi, Y. Kozono, H. Ishida, S. Abe, N. Suzuki, Y. Tsunoda, K. Hagiwara, A. Kuno, T. Ohkura, N. Sato, T. Sato, J. Hirabayashi, Y. Ikehara, K. Tachibana, H. Narimatsu, Polylactosamine on glycoproteins influences basal levels of lymphocyte and macrophage activation, Proc. Natl. Acad. Sci. U.S.A. 104 (2007) 15829–15834.

[10] Q. Sun, X. Kang, Y. Zhang, H. Zhou, Z. Dai, W. Lu, X. Zhou, X. Liu, P. Yang, Y. Liu, DSA affinity glycoproteome of human liver tissue, Arch. Biochem. Biophys. 484 (2009) 24–29.

[11] J. Gu, T. Isaji, Y. Sato, Y. Kariya, T. Fukuda, Importance of N-glycosylation on alpha5beta1 integrin for its biological functions, Biol. Pharm. Bull. 32 (2009) 780–785.

[12] S. Laferte, J.W. Dennis, Purification of two glycoproteins expressing beta 1–6 branched Asn-linked oligosaccharides from metastatic tumour cells, Biochem. J. 259 (1989) 569–576.

[13] W. Tang, S.B. Chang, M.E. Hemler, Links between CD147 function, glycosylation, and caveolin-1, Mol. Biol. Cell 15 (2004) 4043–4050.

[14] R. Chen, X. Jiang, D. Sun, G. Han, F. Wang, M. Ye, L. Wang, H. Zou, Glycoproteomics analysis of human liver tissue by combination of multiple enzyme digestion and hydrazide chemistry, J. Proteome Res. 8 (2009) 651–661.

[15] T. Liu, W.J. Qian, M.A. Gritsenko, D.G. Camp 2nd, M.E. Monroe, R.J. Moore, R.D. Smith, Human plasma N-glycoproteome analysis by immunoaffinity subtraction, hydrazide chemistry, and mass spectrometry, J. Proteome Res. 4 (2005) 2070–2080.

[16] B. Wollscheid, D. Bausch-Fluck, C. Henderson, R. O'Brien, M. Bibel, R. Schiess, R. Aebersold, J.D. Watts, Mass-spectrometric identification and relative quantification of N-linked cell surface glycoproteins, Nat. Biotechnol. 27 (2009) 378–386.

[17] Y. Yan, S. Vasudevan, H.T. Nguyen, D. Merlin, Intestinal epithelial CD98: an oligomeric and multifunctional protein, Biochim. Biophys. Acta 1780 (2008) 1087–1092.

[18] J.Y. Cho, D.A. Fox, V. Horejsi, K. Sagawa, K.M. Skubitz, D.R. Katz, B. Chain, The functional interactions between CD98, beta1-integrins, and CD147 in the induction of U937 homotypic aggregation, Blood 98 (2001) 374–382.

[19] H.B. Guo, I. Lee, M. Kamar, S.K. Akiyama, M. Pierce, Aberrant N-glycosylation of beta1 integrin causes reduced alpha5beta1 integrin clustering and stimulates cell migration, Cancer Res. 62 (2002) 6837–6845.

[20] L. Li, C.J. Fang, J.C. Ryan, E.C. Niemi, J.A. Lebron, P.J. Bjorkman, H. Arase, F.M. Torti, S.V. Torti, M.C. Nakamura, W.E. Seaman, Binding and uptake of H-ferritin are mediated by human transferrin receptor-1, Proc. Natl. Acad. Sci. U.S.A. 107 (2010) 3505–3510.

[21] O. Saitoh, W.C. Wang, R. Lotan, M. Fukuda, Differential glycosylation and cell surface expression of lysosomal membrane glycoproteins in sublines of a human colon cancer exhibiting distinct metastatic potentials, J. Biol. Chem. 267 (1992) 5700–5711.

[22] S.R. Carlsson, J. Roth, F. Piller, M. Fukuda, Isolation and characterization of human lysosomal membrane glycoproteins, h-lamp-1 and h-lamp-2. Major sialoglycoproteins carrying polylactosaminoglycan, J. Biol. Chem. 263 (1988) 18911–18919.

[23] L.C. Bordador, X. Li, B. Toole, B. Chen, J. Regezi, L. Zardi, Y. Hu, D.M. Ramos, Expression of emmprin by oral squamous cell carcinoma, Int. J. Cancer 85 (2000) 347–352.

[24] K. Nabeshima, J. Suzumiya, M. Nagano, K. Ohshima, B.P. Toole, K. Tamura, H. Iwasaki, M. Kikuchi, Emmprin, a cell surface inducer of matrix metalloproteinases (MMPs), is expressed in T-cell lymphomas, J. Pathol. 202 (2004) 341–351.

[25] R. Sawada, J.B. Lowe, M. Fukuda, E-selectin-dependent adhesion efficiency of colonic carcinoma cells is increased by genetic manipulation of their cell surface lysosomal membrane glycoprotein-1 expression levels, J. Biol. Chem. 268 (1993) 12675–12681.

[26] F. Esteban, F. Ruiz-Cabello, A. Concha, M. Perez Ayala, M. Delgado, F. Garrido, Relationship of 4F2 antigen with local growth and metastatic potential of squamous cell carcinoma of the larynx, Cancer 66 (1990) 1493–1498.

[27] S. Esseghir, J.S. Reis-Filho, A. Kennedy, M. James, M.J. O'Hare, R. Jeffery, R. Poulsom, C.M. Isacke, Identification of transmembrane proteins as potential prognostic markers and therapeutic targets in breast cancer by a screen for signal sequence encoding transcripts, J. Pathol. 210 (2006) 420–430.

[28] K. Kaira, N. Oriuchi, H. Imai, K. Shimizu, N. Yanagitani, N. Sunaga, T. Hisada, S. Tanaka, T. Ishizuka, Y. Kanai, H. Endou, T. Nakajima, M. Mori, l-type amino acid transporter 1 and CD98 expression in primary and metastatic sites of human neoplasms, Cancer Sci. 99 (2008) 2380–2386.

[29] G.W. Prager, M. Poettler, M. Schmidinger, P.R. Mazal, M. Susani, C.C. Zielinski, A. Haitel, CD98hc (SLC3A2), a novel marker in renal cell cancer, Eur. J. Clin. Invest. 39 (2009) 304–310.

[30] M. Amano, M. Galvan, J. He, L.G. Baum, The ST6Gal I sialyltransferase selectively modifies N-glycans on CD45 to negatively regulate galectin-1-induced CD45 clustering, phosphatase modulation, and T cell death, J. Biol. Chem. 278 (2003) 7469–7475.

[31] D.W. Ohannesian, D. Lotan, R. Lotan, Concomitant increases in galectin-1 and its glycoconjugate ligands (carcinoembryonic antigen, lamp-1, and lamp-2) in cultured human colon carcinoma cells by sodium butyrate, Cancer Res. 54 (1994) 5992–6000.

[32] K. Yamashita, K. Totani, M. Kuroki, Y. Matsuoka, I. Ueda, A. Kobata, Structural studies of the carbohydrate moieties of carcinoembryonic antigens, Cancer Res. 47 (1987) 3451–3459.

[33] A. Engering, L. Kuhn, D. Fluitsma, E. Hoefsmit, J. Pieters, Differential post-translational modification of CD63 molecules during maturation of human dendritic cells, Eur. J. Biochem. 270 (2003) 2412–2420.

[34] M.S. Kwon, S.H. Shin, S.H. Yim, K.Y. Lee, H.M. Kang, T.M. Kim, Y.J. Chung, CD63 as a biomarker for predicting the clinical outcomes in adenocarcinoma of lung, Lung Cancer 57 (2007) 46–53.

analytical chemistry

Article

pubs.acs.org/ac

Analysis of Nonhuman *N*-Glycans as the Minor Constituents in Recombinant Monoclonal Antibody Pharmaceuticals

Eiki Maeda,[†] Soichiro Kita,[‡] Mitsuhiro Kinoshita,[‡] Koji Urakami,[†] Takao Hayakawa,[§] and Kazuaki Kakehi*[,‡]

[†]Analytical Development Laboratories, CMC Center, Takeda Pharmaceutical Company Limited, Jusohonmachi 2-17-85, Yodogawa-ku, Osaka 532-8686, Japan

[‡]Faculty of Pharmaceutical Sciences, and [§]Pharmaceutical Research and Technology Institute, Kinki University, Kowakae 3-4-1, Higashi-Osaka 577-8502, Japan

Supporting Information

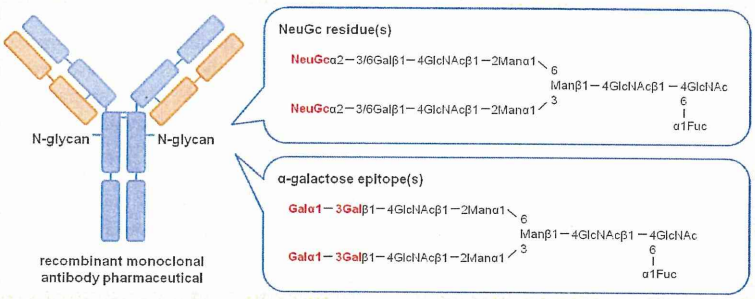

ABSTRACT: Minor N-linked glycans containing *N*-glycolylneuraminic acid residues and/or α-Gal epitopes (i.e., galactose-α1,3-galactose residues) have been reported to be present in recombinant monoclonal antibody (mAb) therapeutics. These contaminations are due to their production processes using nonhuman mammalian cell lines in culture media containing animal-derived materials. In case of the treatment of tumors, we inevitably use such mAbs by careful risk−benefit considerations to prolong patients' lives. However, expanding their clinical applications such as for rheumatism, asthma, and analgesia demands more careful evaluation of the product characteristics. The present work for detailed evaluations of *N*-glycans demonstrates the methods using capillary electrophoresis with laser-induced fluorescence detection (CE-LIF) and a combination of high-performance liquid chromatography and electrospray ionization time-of-flight mass spectrometry. The CE-LIF method provides excellent separation of both major and minor *N*-glycans from six commercial mAb pharmaceuticals within 30 min and clearly indicates that a possible trigger of immunogenicity in humans due to the presence of nonhuman *N*-glycans is present. We strongly believe that the proposed method will be a powerful tool for the analysis of *N*-glycans of recombinant mAb products in various development stages, such as clone selection, process control, and routine release testing to ensure safety and efficacy of the products.

Therapeutic recombinant monoclonal antibodies (mAbs) normally contain several N-linked glycans at asparagine residues on heavy chains.[1] The attached *N*-glycans play important biological and physicochemical roles such as resistance against protease, elongation of circulatory half-life in vivo, and antibody-dependent cellular cytotoxicity.[2−6] Although the attached *N*-glycans are mostly biantennary and core-fucosylated complex-type, their composition usually varies with the changes in manufacturing process conditions even if the same cell line is used.[7−10] In order to ensure quality of the mAb pharmaceuticals, all the *N*-glycans have to be analyzed as a critical parameter for product characterization and lot-to-lot consistency assessment.

Determination of nonhuman *N*-glycans that are not present in humans is especially important, because this will be a big problem in relation to immunogenicity and possible factor for incidence of some diseases, and possible masking of existing antigenic sites on the peptide backbone causes a crucial side effect or insufficient efficacy.[11] Recently, some important research works on the presence of nonhuman *N*-glycans in mAb products were reported. The one is galactose-α1,3-galactose (known as α-Gal epitope) attached to the non-reducing terminal of *N*-glycans. Chung et al. reported that cetuximab, a chimeric mouse−human IgG_1 mAb against the epidermal growth factor receptor produced in murine myeloma SP2/0 cell line, induced hypersensitivity reactions to subjects having IgE antibodies specific for α-Gal epitope on the Fab portion of the cetuximab heavy chain.[12] This epitope is not biosynthesized in old world monkeys, apes, humans, and CHO

Received: November 24, 2011
Accepted: February 13, 2012
Published: February 13, 2012

cells because of inactivation of the gene coding for α-1,3-galactosyltransferase (EC 2.4.1.151).[12−15] Other isotypes against the same epitope are also reported, such as IgG antibodies in serum (approximately 20−100 μg/mL) and also IgA antibodies in body secretions from saliva, milk, and colostrum.[16−18] It is now recognized that the epitope is one of the major barriers in the transplantation of organs from other mammals to humans because of inducing complement-mediated destruction and antibody-dependent cell-mediated destruction.[19,20] The other is the presence of *N*-glycolylneuraminic acid (NeuGc) residues attached to the nonreducing terminal of *N*-glycans. NeuGc cannot be synthesized in humans either, because of an irreversible mutation of the human gene *CMAH*, encoding CMP-*N*-acetylneuraminic acid hydroxylase, which is responsible for producing CMP-*N*-glycolylneuraminic acid from CMP-*N*-acetylneuraminic acid.[21,22] NeuGc exists in almost all animal cells but is not found in human tissues.[23] In several controversial reports published previously, small amounts of NeuGc have been claimed to exist in fetal human tissue, certain human tumors, and human tumor cell lines.[24,25] Normal humans have variable amounts of circulating IgA, IgM, and IgG antibodies against Neu5Gc.[26,27] Recently, Ghaderi et al. demonstrated the presence of covalently bound NeuGc in a therapeutic mAb, cetuximab, but not in panitumumab. Anti-NeuGc antibodies from healthy humans interacted with cetuximab in a NeuGc-specific manner and generated immune complexes in vitro. In addition, mice having a human-like defect in NeuGc synthesis generated antibodies to NeuGc after injection of cetuximab, and circulating anti-NeuGc antibodies can promote drug clearance.[28] These findings relevant to nonhuman *N*-glycans containing α-Gal epitopes and NeuGc residues are considered as warnings against pharmaceutical companies which have been developing therapeutic mAb pharmaceuticals.

The combination of high-performance liquid chromatography (HPLC) coupled with mass spectrometry and endoglycosidase digestion provides sufficient resolution and sensitivity for *N*-glycans.[29−34] In addition, capillary electrophoresis with laser-induced fluorescence detection (CE-LIF) has also been used for profiling of the fluorescently labeled *N*-glycans because of its throughput and high-resolution separation capability.[7,8,33−38] Chen et al. reported structural analysis of *N*-glycans of ribonuclease B, fetuin, and erythropoietin by CE-LIF after fluorescent labeling with 8-aminopyren-1,3,6-trisulfonate (APTS).[33] APTS-labeled *N*-glycans of mAbs, namely, asialo 0, 1, or 2 galactosylated biantennary complex-type *N*-glycans, were also reported.[34,36] Not only the separation methodologies described above, but also the labeling strategies of glycans for introducing a chromophore or fluorophore to the glycans with recent developments and advances of the glycan analysis, have also been published.[39−41] In the previous study, we developed an *N*-glycan profiling method for therapeutic mAb products using CE-LIF with 2-aminobenzoic acid (2-AA) as a fluorescent tag.[8] By comparison of migration times with those of 2-AA-derivatized *N*-glycans of which structures had been determined by a combination of HPLC and matrix-assisted laser desorption/ionization time-of-flight mass spectrometry (MALDI-TOF MS), all the *N*-glycans including minor species from rituximab were identified.

In the present study, we determined nonhuman *N*-glycans, the possible antigenic carbohydrate epitopes like α-Gal and NeuGc, in commercially available mAb pharmaceuticals in a detailed structural and quantitative manner using CE-LIF and a combination of HPLC and high-resolution time-of-flight mass spectrometry equipped with an electrospray ionization source and hybrid ion trap (LC/ESI-IT-TOF MS). To determine the interproduct variety of their minor *N*-glycans, chimeric Fab−human IgG_1 (cetuximab and infliximab), mouse CDR−human IgG_1 and IgG_4 (tocilizumab, bevacizumab, and gemtuzumab ozogamicin), and human IgG_1 (adalimumab) were selected and investigated. Furthermore, a lot-to-lot repetitive analysis was performed using three different lots of gemtuzumab ozogamicin in order to evaluate intraproduct variation. From the results obtained in this study, we strongly suggest that careful considerations are essentially required for assuring safety and efficacy of the therapeutic recombinant mAb products even if they are fully humanized proteins.

EXPERIMENTAL SECTION

Materials. Therapeutic mAb pharmaceuticals, cetuximab, infliximab, gemtuzumab ozogamicin, tocilizumab, bevacizumab, and adalimumab were donated from Kinki University Nara Hospital. γ-Globulins (human: from Cohn fraction II, III) as a human IgG antibody were purchased from Sigma (St. Louis, MO, U.S.A.). Each mAb preparation was dialyzed against distilled water for 3 days, with changing water several times at 4 °C using cellulose membrane tubing (Sanko Junyaku, Chiyoda-ku, Tokyo, Japan), and then freeze-dried. Other reagents and solvents are described in the Supporting Information.

Preparation of 2-AA-Labeled *N*-Glycans. The released *N*-glycans mixture was labeled with 2-AA according to the method reported previously.[8] After the purification of 2-AA-labeled *N*-glycans by a Sephadex LH-20 column, the collected fluorescent fraction was dried and redissolved in water (100 μL), and a portion were used for further analyses (procedures are described in the Supporting Information).

Structural Determination of the Fractionated *N*-Glycans by LC/ESI-IT-TOF MS. Structures of the *N*-glycans were analyzed by LC/ESI-IT-TOF MS (Shimadzu, Kyoto, Japan). Liquid chromatography was conducted with a CBM-20A system controller, two LC-20AD pumps, an SIL-20AC autosampler, and a CTO-20A column oven (Shimadzu). Chromatographic separation was done with a $5C_{18}$-PAQ (2.0 mm i.d. × 150 mm length, Nacalai Tesque, Kyoto, Japan) at 45 °C using a linear gradient formed by 5% acetonitrile containing 0.1% formic acid (solvent A) and 95% acetonitrile containing 0.1% formic acid (solvent B) at 0.2 mL/min. The column was initially equilibrated and eluted with 97% solvent A for 2 min, from which point solvent B was increased to 25% over 20 min and kept at this composition for additional 5 min. LC/ESI-IT-TOF MS was operated in data-dependent tandem mass spectrometry (MS/MS) mode. The curved desolvation line temperature, heat block temperature, detection voltage, and nebulizer gas flow rate were set at 200 °C, 200 °C, 1.7 kV, and 1.5 L/min, respectively. Data were collected for 80 ms for MS mode and 150 ms for MS/MS mode.

Tandem Mass Spectrometry Analysis for α-Gal-Containing *N*-Glycans by MALDI-QIT-TOF MS. For confirmation of the *N*-glycan structure containing α-Gal epitope, tandem mass analyses were conducted for several *N*-glycans by MALDI-quadrupole ion trap (QIT)-TOF mass spectrometry. MALDI-QIT-TOF mass spectra were acquired on an AXIMA-QIT-TOF mass spectrometer (Shimadzu). A nitrogen laser was used to irradiate samples, and an average shot of 50 times was taken. Argon was used for collision-

induced dissociation. The instrument was operated in positive and reflectron mode. An aqueous sample solution (2 μL) was mixed with a matrix solution (2 μL) of 1% DHB in ethanol/water (1:1), and the mixture was applied to a polished stainless-steel target and dried in atmosphere for a few hours.

CE-LIF of 2-AA-Labeled *N*-Glycans. CE-LIF was performed on a P/ACE MDQ system (Beckman Coulter, Fullerton, CA, U.S.A.) equipped with a He–Cd laser-induced fluorescence detector (ex 325 nm, em 405 nm) using a DB-1 capillary (100 μm i.d., 30 cm effective length, 40 cm total length, Agilent/J&D Scientific, Palo Alto, CA, U.S.A.) in 100 mM Tris–borate buffer (pH 8.3) containing 5% poly(ethylene glycol) as a running buffer. Poly(ethylene glycol) was added to diminish electroosmotic flow and improve the resolution. For pressure injection, sample solutions were introduced to the capillary at 1 psi for 10 s. Separation was performed at 25 kV of applied voltage at 25 °C in reverse polarity.

RESULTS AND DISCUSSION

Structural Analysis of 2-AA-Labeled *N*-Glycans by LC/ESI-IT-TOF MS and MALDI-QIT-TOF MS. The 2-AA-labeled *N*-glycans from six recombinant mAb products and a human IgG antibody were analyzed by HPLC (Figure 1), and the assigned structures of the *N*-glycans from each peak by LC/ESI-IT-TOF MS are listed on each chromatogram and summarized in Table S-1 in the Supporting Information. In total, 46 *N*-glycans were determined from the tested products. Biantennary *N*-glycans **3**, **4**, and **6** were commonly detected as major *N*-glycans in all the products, and their singly charged deprotonated molecules $[M - H]^-$ in gemtuzumab ozogamicin were observed at *m/z* 1582.6, 1744.6, and 1906.7, respectively (Table S-1 in the Supporting Information). Although agalactosylated biantennary *N*-glycan **3** was commonly observed abundantly in all products, mono- and digalactosylated biantennary *N*-glycans **4** and **6** were significantly low in bevacizumab (Figure 1c) and adalimumab (Figure 1f). In addition, the amount of digalactosylated biantennary *N*-glycan **6** in tocilizumab (Figure 1b) and cetuximab (Figure 1d) was much smaller than other mAb products, although they contained a similar amount of monogalactosylated biantennary *N*-glycan **4**. These results indicate that the variety of major *N*-glycans is remotely related to the humanization levels of mAb products.

For minor *N*-glycans (see also the enlarged chromatograms in Figure 1), tocilizumab (Figure 1b) and adalimumab (Figure 1f) contained relatively larger amounts of high-mannose-type *N*-glycans **13–17**, and cetuximab (Figure 1d) and infliximab (Figure 1e) contained larger amounts of hybrid-type *N*-glycans **18–23**, respectively. Sialylated *N*-glycans **24–45** were commonly observed in all mAb products. Interestingly, it was revealed that the major sialylated *N*-glycans of three mAb pharmaceuticals [gemtuzumab ozogamicin (Figure 1a), cetuximab (Figure 1d), and infliximab (Figure 1e)] were occupied with NeuGc residue **33–41**, **45** as identified from the results of LC/ESI-IT-TOF MS (Figure 2). Two doubly charged deprotonated molecules $[M - 2H]^{2-}$ at *m/z* 1098.3 (Figure 2a) and *m/z* 1106.3 (Figure 2b) due to *N*-glycans **26** and **36** were observed in gemtuzumab ozogamicin. Both molecules provided the same singly charged deprotonated molecule $[M - H]^-$ corresponding to digalactosylated biantennary *N*-glycan **6** in their MS/MS spectra (Figure S-1, parts a and b, in the Supporting Information). The calculated mass difference between *N*-glycans **26** and **36** was 16.0, and this clearly

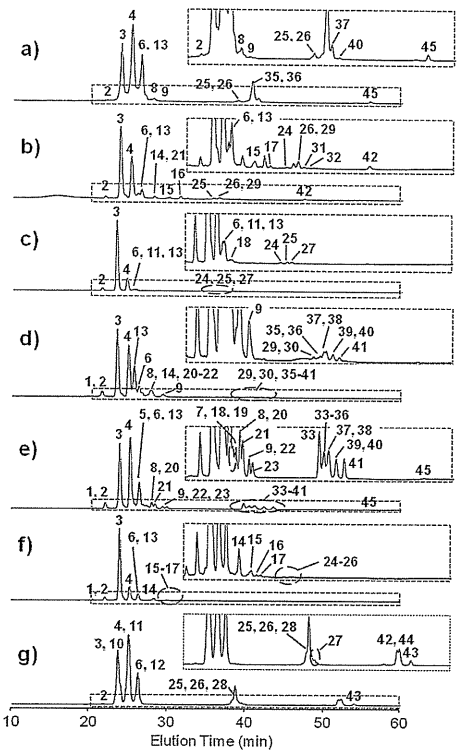

Figure 1. Analysis of 2-AA-labeled *N*-glycans by HPLC: (a) gemtuzumab ozogamicin, (b) tocilizumab, (c) bevacizumab, (d) cetuximab, (e) infliximab, (f) adalimumab, and (g) human IgG antibody. The numbers represent the *N*-glycans observed in each peak, and their structures are summarized in Table S-1 in the Supporting Information. In the box, the region between 20 and 60 min is enlarged. Analytical conditions: column, Asahi Shodex NH2P-50 4E (4.6 mm i.d. × 250 mm length); eluent, solvent A, 2% acetic acid in acetonitrile, solvent B, 5% acetic acid containing 3% triethylamine in water; gradient condition, a linear gradient (30–95% solvent B) from 2 to 82 min, keep for 15 min (95% solvent B); detection, ex 350 nm, em 425 nm.

indicated the presence of NeuGc in gemtuzumab ozogamicin. Not only gemtuzumab ozogamicin manufactured in NS0 murine myeloma cell line, but chimeric antibodies, infliximab and cetuximab, produced in murine myeloma SP2/0 cell lines, also contained NeuGc residues instead of NeuAc. The results are consistent with both the results of sialic acid analysis (see the Supporting Information) and the previous report that cetuximab has NeuGc residues at the nonreducing terminal of *N*-glycans on its Fab region.[28] In contrast, human IgG antibody and other three therapeutic mAbs manufactured in CHO cell lines, tocilizumab, bevacizumab, and adalimumab, did not contain NeuGc-containing *N*-glycans.

Two peaks (**8** and **9**) observed at 28.0 and 29.4 min in gemtuzumab ozogamicin (Figure 1a) provided doubly charged deprotonated molecules $[M - 2H]^{2-}$ at *m/z* 1033.9 (Figure 2c) and *m/z* 1115.3 (Figure 2d), respectively. The structures of these peaks were easily assigned as follows. The mass differences (Δ162.2 and Δ324.1) from digalactosylated biantennary *N*-glycan **6** indicated the presence of additional hexose molecule(s) compared to the *N*-glycan **6**. This means that one or two molecules of galactose attach to the nonreducing ends of *N*-glycan **6** to form one or two α-Gal

dx.doi.org/10.1021/ac300234a | *Anal. Chem.* 2012, 84, 2373–2379

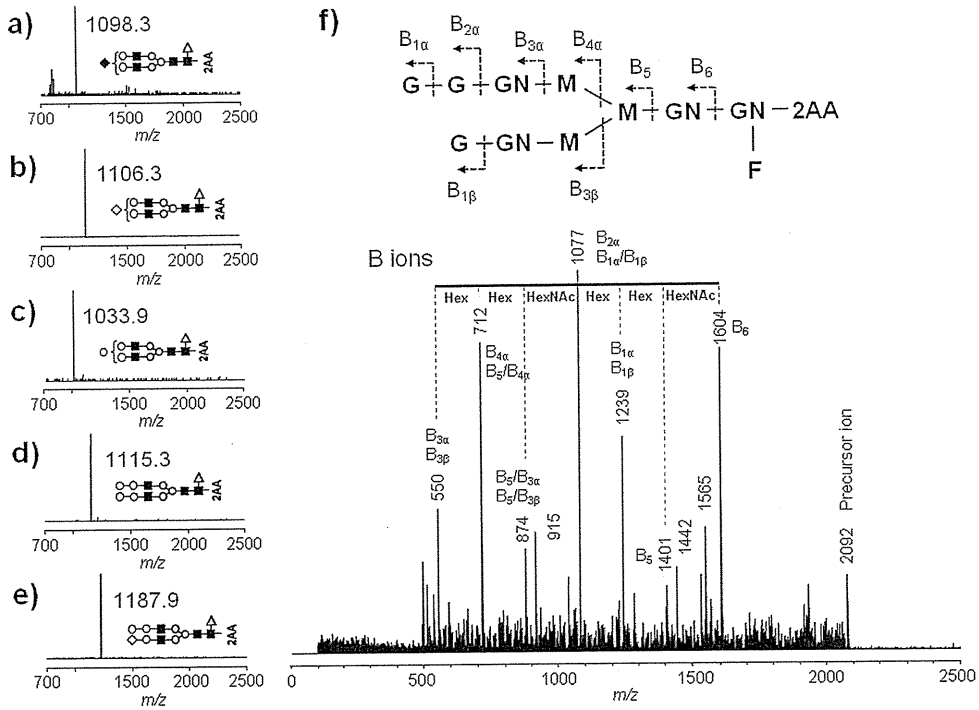

Figure 2. Negative MS spectra and positive MS/MS spectrum of 2-AA-labeled *N*-glycans from gemtuzumab ozogamicin: (a) *N*-glycan **26** containing one NeuAc residue, (b) *N*-glycan **36** containing one NeuGc residue, (c) *N*-glycan **8** containing one α-Gal epitope, (d) *N*-glycan **9** containing two α-Gal epitopes, (e) *N*-glycan **37** containing one NeuGc residue and one α-Gal epitope, and (f) *N*-glycan **8**. The dotted lines on the MS/MS spectrum indicate the type of cleavage according to Domon and Costello's nomenclature (ref 45).

epitopes. In addition, the peak detected at 41.4 min (Figure 1a) showed doubly charged deprotonated molecules $[M - 2H]^{2-}$ at *m/z* 1187.9 (Figure 2e) due to *N*-glycan **37**, and the ion provided singly charged ion $[M - H]^-$ at *m/z* 2069.8 (Figure S-1c in the Supporting Information) corresponding to *N*-glycan **8** by MS/MS analysis. These galactose residues at the nonreducing ends of *N*-glycans were specifically released by enzymatic digestion with α-galactosidase (data not shown). In addition, MS/MS analysis by MALDI-QIT-TOF MS demonstrated the presence of α-Gal epitope in its structure. Figure 2f shows the positive MS/MS spectrum of *N*-glycan **8** corresponding to the peak observed at 28.0 min in Figure 1a. The positive MS/MS spectrum derived from precursor ion $[M + Na]^+$ (*m/z* 2092.0) was mainly consisted by B-type fragment ions. The characteristic B ions at *m/z* 1401.0 (B5) and 1604.0 (B6) corresponding to a loss of 691 and 488 from $[M + Na]^+$ were observed. These mass differences corresponded to a loss of two *N*-acetylhexosamine (HexNAc) residues having a fucose residue with 2-AA and a HexNAc residue having a fucose residue with 2-AA, respectively. This result indicates that the B5 ion at 1401.0 contains three mannose and two HexNAc residues with additional three residues of hexose at the nonreducing end of *N*-glycan. The same fragment ions were observed in other mAb products as well (data not shown). These results obtained by MALDI-QIT-TOF MS obviously show the presence of α-Gal epitope in *N*-glycan **8**.

From the results described above, gemtuzumab ozogamicin contains nonhuman *N*-glycan having α-Gal epitope in its structure. Cetuximab and infliximab also contained these *N*-glycans as well (see Table S-1 in the Supporting Information), and both mAb products induced anaphylaxis mediated by IgE antibody which binds to α-Gal epitope specifically.[12,42] For infliximab, the mechanism of the anaphylaxis is under discussion, but the obtained results indicate that the presence of α-Gal epitope seems to be one of the root causes of the anaphylactic response.

The combination of HPLC and MS provides lots of structural information concerning attached *N*-glycans having NeuGc residues and α-Gal epitopes. However, due to incomplete resolution of the peaks as shown in Figure 1, detailed quantitative analysis of the *N*-glycans is a hard work. For example, two *N*-glycans, digalactosylated biantennary *N*-glycan **6** and high-mannose-type *N*-glycan **13**, which were supposed to be present in almost all mAb products, were observed at the same elution time.

CE-LIF Analysis of 2-AA-Labeled *N*-Glycans. 2-AA-labeled *N*-glycans from mAb products were analyzed by CE-LIF according to the method reported previously (Figure 3).[8] All peaks observed in each electropherogram were assigned using HPLC eluents by comparing migration times. CE-LIF provides much higher resolution than HPLC, and the *N*-glycans were observed in the order of disialo-, monosialo-, high-mannose-type, hybrid-type, and biantennary complex-type asialo-*N*-glycans. It should be noted that the *N*-glycans having the same molecular weight such as monogalactosylated biantennary complex-type *N*-glycans **4** were resolved into two peaks as indicated by asterisks in Figure 3a (at 22.3 and 22.6 min, respectively) depending on the linkage position of galactose residues at the nonreducing end. In addition, as shown in Figure 3b, digalactosylated biantennary complex-type *N*-glycan **6** and high-mannose-type *N*-glycan **13**, which could not be separated by HPLC, were completely resolved, and

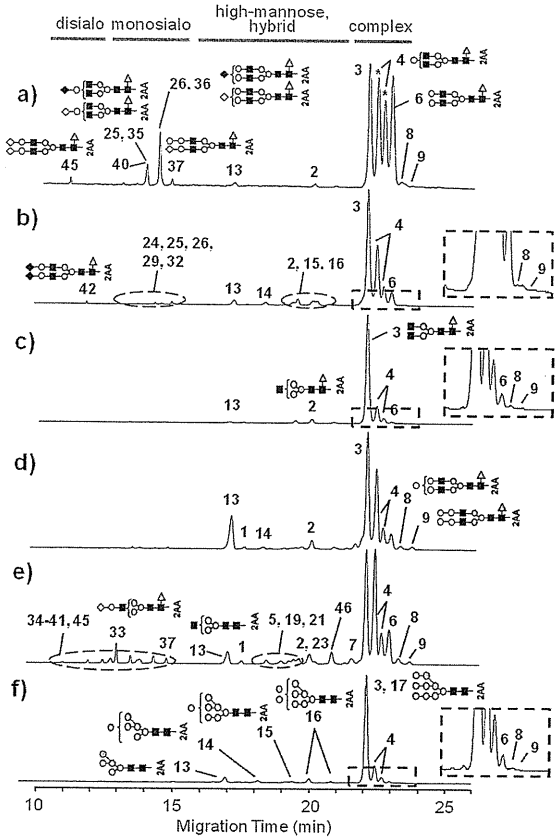

Figure 3. CE-LIF analysis of 2-AA-labeled *N*-glycans: (a) gemtuzumab ozogamicin, (b) tocilizumab, (c) bevacizumab, (d) cetuximab, (e) infliximab, and (f) adalimumab. The numbers represent the *N*-glycans observed in each peak, and their structures are summarized in Table S-1 in the Supporting Information. In the box, the region between 21.5 and 24.0 min is enlarged. Analytical conditions: capillary, DB-1 capillary (100 μm i.d., 30 cm effective length, 40 cm total length); running buffer, 100 mM Tris–borate buffer (pH 8.3) containing 5% PEG70000; injection, 1 psi for 10 s; applied voltage, −25 kV; temperature, 25 °C; detection, ex 325 nm, em 405 nm.

observed at quite different migration times. These results definitely demonstrate that CE-LIF is much more suitable for *N*-glycan profiling than HPLC because of its speed, throughput, and resolution.

From the electropherogram of gemtuzumab ozogamicin, two characteristic peaks were observed at 23.1 and 23.5 min (**8** and **9**, respectively) after four major peaks around 22 min (Figure 3a). These two peaks were observed in all the tested products but not observed in the previous study.[8] By peak assignment using fractionated HPLC eluents of gemtuzumab ozogamicin, these two peaks were identified as *N*-glycans having one and two α-Gal epitopes, respectively (Figure S-3 in the Supporting Information). In the same manner, biantennary complex-type *N*-glycans having one or two NeuGc or NeuAc residues at the nonreducing end (*N*-glycans **25**, **26**, **35**, **36**, and **45**) and hybrid-type *N*-glycan **40** containing a NeuGc residue at the nonreducing ends were also identified (Figure S-3 in the Supporting Information). However, complete separation between *N*-glycans **25** and **35** was not achieved even if using CE-LIF, because their structural difference is only the attached sialic acid types at the nonreducing end, namely, NeuGc or NeuAc. For the same reason, *N*-glycans **26** and **36** were not resolved from each other. For distinguishing terminal sialic acid species, both commonly used separation techniques in the pharmaceutical industry,[43] i.e., HPLC and CE, could not provide a complete separation because *N*-glycans usually contain six or more monosaccharides and the structural difference between NeuGc and NeuAc is much smaller (Δ16.0) than those of total masses. Terminal sialic acid modification could be alternatively accessed by sialic acid analysis, and the dominant types were over 93% as described in the Supporting Information. Therefore, we believe that current CE-LIF method is quite useful for rapid and extensive evaluation of nonhuman *N*-glycans of mAb pharmaceuticals.

The peak identification of nonhuman *N*-glycans containing NeuGc (**33**–**41** and **45**) at the nonreducing end from infliximab was also conducted by using fractionated eluents by HPLC (Figure S-4 in the Supporting Information). All the *N*-glycans having NeuGc (summarized in Table S-1 in the Supporting Information) were detected from infliximab, although one of them (*N*-glycan **39**) could not be observed by LC/ESI-IT-TOF MS. Separation between hybrid-type *N*-glycans **40** and monogalactosylated biantennary complex-type *N*-glycans **35** was achieved. The results obtained by CE-LIF indicate that the CE-LIF method affords good separation of over 40 *N*-glycans within 30 min, and the method can be used as a rapid *N*-glycan profiling in several development stages of therapeutic recombinant mAbs for monitoring and controlling product consistency as well as assuring safety and efficacy of the products.

Quantitative CE-LIF Analysis of 2-AA-Labeled *N*-Glycans. The percent compositions of detected *N*-glycans in each mAb product are summarized in Table 1. Three major *N*-glycans, **3**, **4**, and **6**, in gemtuzumab ozogamicin, tocilizumab,

Table 1. Quantitative Analysis of Attached *N*-Glycans in Recombinant mAb Products

	sialo- (%)			complex-type (%)					
product[a]	type	di-	mono-	**3**	**4**	**4**	**6**	**8, 9**	others (%)[b]
gem	NeuGc	0.4	8.9	23.9	23.1	17.5	22.1	2.3	1.8
toc	NeuAc	0.3	1.7	47.8	24.2	7.6	5.9	0.8	11.6
bev	NeuAc	0.0	0.3	75.5	12.7	3.7	1.3	1.7	6.1
cet	NeuGc	0.1	1.0	37.5	26.1	7.0	5.5	2.3	20.6
inf	NeuGc	0.1	7.4	27.6	28.7	7.9	9.0	2.4	17.1
ada	NeuAc	0.0	0.4	71.2	11.9	4.0	1.1	0.3	10.9
hIgG	NeuAc	0.6	11.1	37.8	22.7	10.9	14.0	0.0	2.9

[a]Symbols: gem, gemtuzumab ozogamicin; toc, tocilizumab; bev, bevacizumab; cet, cetuximab; inf, infliximab; ada, adalimumab; hIgG, human IgG antibody. [b]High-mannose-type and hybrid-type *N*-glycans.

dx.doi.org/10.1021/ac300234a | *Anal. Chem.* 2012, 84, 2373–2379

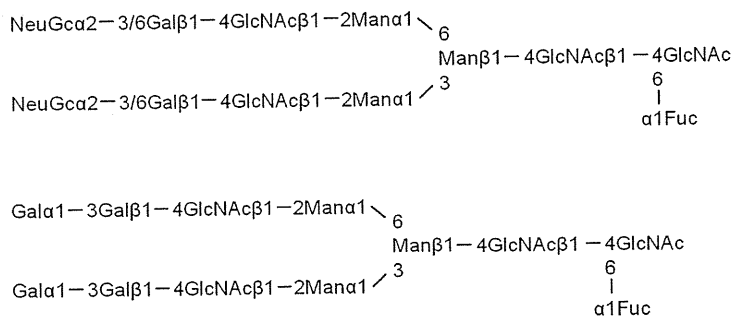

Figure 4. Representative scheme of nonhuman *N*-glycans containing NeuGc residues (a) and α-Gal epitopes (b).

bevacizumab, cetuximab, infliximab, adalimumab, and human IgG antibody (as the standard) occupied 86.6%, 85.5%, 93.2%, 76.1%, 73.2%, 88.2%, and 85.4%, respectively. For agalactosylated biantennary *N*-glycan **3**, the range of the compositions was varied from 23.9% to 75.5%. For the two peaks due to monogalactosylated biantennary complex-type *N*-glycans **4** which could be separated into two peaks, the earlier detected molecule showed a higher percent composition than the latter one in all the products. For example, these were 23.1% and 17.5% in gemtuzumab ozogamicin, respectively.

The percent compositions of minor *N*-glycans showed higher diversity than those observed for major peaks. For example, tocilizumab, cetuximab, infliximab, and adalimumab contained over 10% of high-mannose-type and hybrid-type *N*-glycans. Gemtuzumab ozogamicin and infliximab contained over 7% of monosialylated *N*-glycans of which sialic acids were exclusively NeuGc. It should be noted that all the mAb products examined in the present study except for human IgG antibody have nonhuman *N*-glycans containing α-Gal epitope(s) (**8** and **9**) as examined by CE-LIF. Again, we would like to emphasize that careful considerations are strongly needed not only for types of *N*-glycans but also for the amounts of each *N*-glycan, especially having nonhuman constituents like NeuGc residue and α-Gal epitope in their structure. It should be also emphasized that this is conveniently achieved by CE-LIF method.

Lot-to-Lot Variation of *N*-Glycan Distribution. In order to address the intraproduct variations of attached *N*-glycans, lot-to-lot analysis was performed using three different lots of gemtuzumab ozogamicin as a model mAb product. Relative standard deviations (RSDs) of percent compositions for major *N*-glycans **3**, **4**, and **6** were not higher than 2.3%, and it showed that good consistency was kept between each lot (summarized in Table S-2 in the Supporting Information). Moreover, for minor *N*-glycans having disialo-, monosialo-, and one or two α-Gal epitope(s) showed reproducible results (RSDs ≤ 5.5%). However, the sum of high-mannose-type and hybrid-type *N*-glycans showed over 10% in RSD values due to their small abundances. From the results described here, the attached *N*-glycans kept constant distributions among the production lots, although they showed wide diversity among the products due to the differences in their manufacturing process.

CONCLUSION

Detailed structural and quantitative analyses of N-linked glycans from six therapeutic recombinant mAb products by CE-LIF and LC/ESI-IT-TOF MS demonstrate their variety due to differences in the manufacturing process, especially cell types. Forty-six *N*-glycans were successfully assigned from the tested mAbs, and they include nonhuman *N*-glycans containing NeuGc residues instead of NeuAc (*N*-glycans **33**–**41** and **45**) and α-Gal epitope(s) (*N*-glycans **8**, **9**, and **37**). The former structure (representative structure is shown in Figure 4a) was observed in three mAb pharmaceuticals produced in nonhuman mammalian cell lines such as murine myeloma SP2/0 and NS0 cell lines, whereas it was absent in other mAbs produced in CHO cell lines. However, even if a CHO cell line is used for the production, NeuGc can be taken up and metabolically incorporated into secreted glycoprotein when animal-derived materials are used as a culture medium during the manufacturing process. Therefore, pharmaceutical companies should have their own strategy to reduce its uptake by adding a human sialic acid (i.e., NeuAc) to the culture medium.[28,44] The latter structure (Figure 4b) was observed in all the tested mAb products by CE-LIF analysis.

It should be noticed that fully humanized mAb, adalimumab, still contains α-Gal epitope. Since the detailed mechanism of this contamination is not clear, further investigation must be necessary in order to reduce or eliminate the risk of crucial side effect or insufficient efficacy in humans. Unfortunately, the detailed correlation between the risks led by these contaminations and the amount of the glycans is not still clear. Furthermore, since the peptide portion to which these nonhuman *N*-glycans are attached is not accessed in this study, it should be verified in a future work on peptide analysis of the mAb pharmaceuticals.

Hyphenated techniques of HPLC/CE with MS are powerful approaches for getting structural information, even if minor glycans are present at low levels. Actually, in tocilizumab, bevacizumab, and adalimumab, the *N*-glycans containing α-Gal epitope are present at very low levels compared to the whole amounts of *N*-glycans. When analyzed by LC/MS, as shown in Figure 1, parts b, c, and f, it was hard to detect these *N*-glycans accurately due to their very low amounts and interference by other *N*-glycans which coeluted in HPLC. In contrast, in CE-LIF, these *N*-glycans, especially *N*-glycans **8** and **9**, could be obviously separated and observed at the end of the run, around 23–24 min, as described in Figure 3, parts b, c, and f, respectively. These results clearly indicate that the CE-LIF method provides notable information regarding the presence of α-Gal epitope in mAb products rather than the HPLC method, from the aspect of glycan analysis. In the glycan analysis of mAb pharmaceuticals, both identity and quantity of nonhuman *N*-glycans are quite important information. For further investigation in order to find out the threshold of the glycan contaminations, the proposed CE-LIF method is quite useful for rapid, quantitative, and extensive evaluations of *N*-glycans of

mAb pharmaceuticals in various development stages such as, for example, clone selection, bioprocess control, detailed characterization for approval application, and lot release testing.

Although the CE/MS method for glycan analysis sounds to be a really appropriate strategy, CE cannot provide sufficient separation of *N*-glycans without the sieving effect by neutral polymers in the separation buffers. This problem leads to less quantitative information in CE/MS analysis. Therefore, when applying CE/MS to a detailed glycan analysis, this discrepancy between "resolutions of glycans" and "obtaining quantitative data" needs to be improved.

The indications of recombinant mAb products have been remarkably expanding into solid tumor, leukemia, rheumatism, asthma, and analgesia. Some of them need long-term drug exposure for obtaining sufficient results. In order to improve safety and efficacy of the products, pharmaceutical companies have to monitor and control the variations of *N*-glycans in their products especially when possible antigenic carbohydrate constituents, NeuGc residue and/or α-Gal epitope, are present, through all the development and clinical stages, even if they are fully humanized products. We believe that the present report will be a useful guide for evaluating attached *N*-glycans of mAb products.

■ ASSOCIATED CONTENT

Supporting Information

Additional information as noted in text. This material is available free of charge via the Internet at http://pubs.acs.org.

■ AUTHOR INFORMATION

Corresponding Author

*Phone: +81-6-6721-2332. Fax: +81-6-6721-2353. E-mail: k_kakehi@phar.kindai.ac.jp.

Notes

The authors declare no competing financial interest.

■ REFERENCES

(1) Sutton, B. J.; Phillips, D. C. *Biochem. Soc. Trans.* **1983**, *11*, 130–132.

(2) Tao, M. H.; Morrison, S. L. *J. Immunol.* **1989**, *143*, 2595–2601.

(3) Flintegaard, T. V.; Thygesen, P.; Rahbek-Nielsen, H.; Levery, S. B.; Kristensen, C.; Clausen, H.; Bolt, G. *Endocrinology* **2010**, *151*, 5326–5336.

(4) Umaña, P.; Jean-Mairet, J.; Moudry, R.; Amstutz, H.; Bailey, J. E. *Nat. Biotechnol.* **1999**, *17*, 176–180.

(5) Shields, R. L.; Lai, J.; Keck, R.; O'Connell, L. Y.; Hong, K.; Meng, Y. G.; Weikert, S. H. A.; Presta, L. G. *J. Biol. Chem.* **2002**, *277*, 26733–26740.

(6) Shinkawa, T.; Nakamura, K.; Yamane, N.; Shoji-Hosaka, E.; Kanda, Y.; Sakurada, M.; Uchida, K.; Anazawa, H.; Satoh, M.; Yamasaki, M.; Hanai, N.; Shitara, K. *J. Biol. Chem.* **2003**, *278*, 3466–3473.

(7) Kamoda, S.; Nomura, C.; Kinoshita, M.; Nishiura, S.; Ishikawa, R.; Kakehi, K.; Kawasaki, N.; Hayakawa, T. *J. Chromatogr., A* **2004**, *1050*, 211–216.

(8) Kamoda, S.; Ishikawa, R.; Kakehi, K. *J. Chromatogr., A* **2006**, *1133*, 332–339.

(9) Mizuochi, T.; Taniguchi, T.; Shimizu, A.; Kobata, A. *J. Immunol.* **1982**, *129*, 2016–2020.

(10) Fujii, S.; Nishiura, T.; Nishikawa, A.; Miura, R.; Taniguchi, N. *J. Biol. Chem.* **1990**, *265*, 6009–6018.

(11) Feizi, T.; Childs, R. A. *Biochem. J.* **1987**, *245*, 1–11.

(12) Chung, C. H.; Mirakhur, B.; Chan, E.; Le, Q.-T.; Berlin, J.; Morse, M.; Murphy, B. A.; Satinover, S. M.; Hosen, J.; Mauro, D.; Slebos, R. J.; Zhou, Q.; Gold, D.; Hatley, T.; Hicklin, D. J.; Platts-Mills, T. A. E. *N. Engl. J. Med.* **2008**, *358*, 1109–1117.

(13) Joziasse, D. H.; Shaper, J. H.; Jabs, E. W.; Shaper, N. L. *J. Biol. Chem.* **1991**, *266*, 6991–6998.

(14) Smith, D. F.; Larsen, R. D.; Mattox, S.; Lowe, J. B.; Cummings, R. D. *J. Biol. Chem.* **1990**, *265*, 6225–6234.

(15) Lantéri, M.; Giordanengo, V.; Vidal, F.; Gaudray, P.; Lefebvre, J.-C. *Glycobiology* **2002**, *12*, 785–792.

(16) Galili, U.; Rachmilewitz, E. A.; Peleg, A.; Flechner, I. *J. Exp. Med.* **1984**, *160*, 1519–1531.

(17) Galili, U. *Springer Semin. Immunopathol.* **1993**, *15*, 155–171.

(18) Galili, U. *Transplantation* **2004**, *78*, 1093–1098.

(19) Macher, B. A.; Galili, U. *Biochim. Biophys. Acta* **2008**, *1780*, 75–88.

(20) Kobayashi, T.; Cooper, D. K. *Subcell. Biochem.* **1999**, *32*, 229–257.

(21) Varki, A. *Nature* **2007**, *446*, 1023–1029.

(22) Hayashi, N.; Kawasaki, N.; Nakajima, Y.; Toyoda, M.; Katagiri, Y.; Itoh, S.; Harazono, A.; Umezawa, A.; Yamaguchi, T. *J. Chromatogr., A* **2007**, *1160*, 263–269.

(23) Nakamura, K.; Ariga, T.; Yahagi, T.; Miyatake, T.; Suzuki, A.; Yamakawa, T. *J. Biochem.* **1983**, *94*, 1359–1365.

(24) Varki, A. *Glycobiology* **1992**, *2*, 25–40.

(25) Marquina, G.; Waki, H.; Fernandez, L. E.; Kon, K.; Carr, A.; Valiente, O.; Perez, R.; Ando, S. *Cancer Res.* **1996**, *56*, 5165–5171.

(26) Tangvoranuntakul, P.; Gagneux, P.; Diaz, S.; Bardor, M.; Varki, N.; Varki, A.; Muchmore, E. *Proc. Natl. Acad. Sci. U.S.A.* **2003**, *100*, 12045–12050.

(27) Padler-Karavani, V.; Yu, H.; Cao, H.; Chokhawala, H.; Karp, F.; Varki, N.; Chen, X.; Varki, A. *Glycobiology* **2008**, *18*, 818–830.

(28) Ghaderi, D.; Taylor, R. E.; Padler-Karavani, V.; Diaz, S.; Varki, A. *Nat. Biotechnol.* **2010**, *28*, 863–867.

(29) Anumula, K. R.; Dhume, S. T. *Glycobiology* **1998**, *8*, 685–694.

(30) Nakano, M.; Kakehi, K.; Tsai, M.-H.; Lee, Y. C. *Glycobiology* **2004**, *14*, 431–441.

(31) Kamoda, S.; Nakano, M.; Ishikawa, R.; Suzuki, S.; Kakehi, K. *J. Proteome Res.* **2005**, *4*, 146–152.

(32) Naka, R.; Kamoda, S.; Ishizuka, A.; Kinoshita, M.; Kakehi, K. *J. Proteome Res.* **2006**, *5*, 88–97.

(33) Chen, F. T.; Evangelista, R. A. *Electrophoresis* **1998**, *19*, 2639–2644.

(34) Ma, S.; Nashabeh, W. *Anal. Chem.* **1999**, *71*, 5185–5192.

(35) Kakehi, K.; Funakubo, T.; Suzuki, S.; Oda, Y.; Kitada, Y. *J. Chromatogr., A* **1999**, *863*, 205–218.

(36) Raju, T. S. *Anal. Biochem.* **2000**, *283*, 125–132.

(37) Nakajima, K.; Oda, Y.; Kinoshita, M.; Kakehi, K. *J. Proteome Res.* **2003**, *2*, 81–88.

(38) Ma, S.; Lau, W.; Keck, R. G.; Briggs, J. B.; Jones, A. J. S.; Moorhouse, K.; Nashabeh, W. *Methods Mol. Biol.* **2005**, *308*, 397–409.

(39) Ruhaak, L. R.; Zauner, G.; Huhn, C.; Bruggink, C.; Deelder, A. M.; Wuhrer, M. *Anal. Bioanal. Chem.* **2010**, *397*, 3457–3481.

(40) Huhn, C.; Selman, M. H. J.; Ruhaak, L. R.; Deelder, A. M.; Wuhrer, M. *Proteomics* **2009**, *9*, 882–913.

(41) Pabst, M.; Kolarich, D.; Pöltl, G.; Dalik, T.; Lubec, G.; Hofinger, A.; Altmann, F. *Anal. Biochem.* **2009**, *384*, 263–273.

(42) Vultaggio, A.; Matucci, A.; Nencini, F.; Pratesi, S.; Parronchi, P.; Rossi, O.; Romagnani, S.; Maggi, E. *Allergy* **2010**, *65*, 657–661.

(43) Read, E. K.; Park, J. T.; Brorson, K. A. *Biotechnol. Appl. Biochem.* **2011**, *58*, 213–219.

(44) Bardor, M.; Nguyen, D. H.; Diaz, S.; Varki, A. *J. Biol. Chem.* **2005**, *280*, 4228–4237.

(45) Domon, B.; Costello, C. E. *Biochemistry* **1988**, *27*, 1534–1543.

Analytical Biochemistry 421 (2012) 595–606

Contents lists available at SciVerse ScienceDirect

Analytical Biochemistry

journal homepage: www.elsevier.com/locate/yabio

One-pot characterization of cancer cells by the analysis of mucin-type glycans and glycosaminoglycans

Keita Yamada [a,b], Yosuke Mitsui [a], Naotaka Kakoi [a], Mitsuhiro Kinoshita [a], Takao Hayakawa [c], Kazuaki Kakehi [a,*]

[a] School of Pharmacy, Kinki University, Higashi-Osaka, Osaka 577-8502, Japan
[b] Division of Glyco-Bioindustry, Life Science Research Center, Institute of Research Promotion, Kagawa University, Miki-cho, Kita-gun, Kagawa 761-0793, Japan
[c] Pharmaceutical Research and Technology Institute, Kinki University, Higashi-Osaka, Osaka 577-8502, Japan

ARTICLE INFO

Article history:
Received 14 September 2011
Received in revised form 5 December 2011
Accepted 8 December 2011
Available online 14 December 2011

Keywords:
Mucin-type glycans
Glycosaminoglycans
Serotonin affinity chromatography
Capillary electrophoresis
MALDI–TOF MS
Cancer cells

ABSTRACT

We developed an automated apparatus for rapid releasing of *O*-glycans from mucin-type glycoproteins [Anal. Biochem. 371 (2007) 52–61; Anal. Chem. 82 (2010) 7436–7443] and applied the device to analyze them in some cancer cell lines [J. Proteome Res. 8 (2009) 521–537]. We also found that the device is useful to release glycosaminoglycans from proteoglycans [Anal. Biochem. 362 (2007) 245–251]. Based on these studies, we developed a method for one-pot analysis of mucin-type glycans and glycosaminoglycans after releasing them from total protein pool obtained from some cancer cell lines. Mucin-type glycans were analyzed by a combination of high-performance liquid chromatography and mass spectrometry techniques, and glycosaminoglycans were analyzed by capillary electrophoresis as fluorescent-labeled unsaturated disaccharides after digestion with specific eliminases followed by fluorescent labeling. Ten cancer cell lines, including blood cancer cells as well as epithelial cancer cells, were used to assess the method. The results clearly revealed that both mucin-type glycans and glycosaminoglycans showed quite interesting profiles. Thus, the current technique will be a powerful tool for discovery of glycan markers of diseases.

Analysis of glycan structures has become one of the requirements of postgenomic research. Most of the glycans attached to glycoproteins are classified into *N*- and *O*-glycans. Because of the extremely complex structures and heterogeneity of both *N*- and *O*-glycans, we often need to analyze their structures after releasing them from the core protein. In the analysis of *N*-glycans, *N*-glycoamidase having broad specificity is generally used to release *N*-glycans from the peptide backbone. We reported two methods for the analysis of *N*-glycans by labeling with 9-fluorenylmethyl chloroformate and 2-aminobenzoic acid (2AA)[1] [1,2]. These two methods allow sensitive analysis of *N*-glycans by high-performance liquid chromatography (HPLC), capillary electrophoresis (CE), and mass spectrometry (MS). We also achieved comprehensive analysis of *N*-glycans in various cancer cell lines and antibody pharmaceuticals [2,3].

In contrast, structural and quantitative analysis of *O*-glycans attached to the mucin-type glycoproteins has been a difficult task due to lack of appropriate *O*-glycan releasing methods. β-Elimination under mild alkaline conditions is still commonly employed but requires long reaction times. In addition, reducing reagents such as sodium borohydride need to be added to prevent unwanted degradation of the released glycans (i.e., peeling) [4–6]. This causes a loss of the original reducing terminal, and the released glycans do not have an aldehyde group, which is important for sensitive detection and high-resolution analysis by labeling with sensitive fluorescent or chromophoric reagents.

Release of *O*-glycans with the intact reducing end has been reported. Royle and coworkers employed mild hydrazinolysis to afford free *O*-glycans from microgram quantities of glycoproteins, but a lengthy reaction time and reacetylation of de-N-acetylated groups are required [7]. Huang and coworkers developed a method for releasing *O*-glycans in the presence of ammonia, but the method also requires a long reaction time [8].

Recently, we developed an automatic *O*-glycan releasing apparatus to obtain *O*-glycans from core proteins as free form. The apparatus enables release of *O*-glycans within only 3 min without significant degradations of the released glycans. In addition, our method showed excellent repeatability [9,10]. We also connected

* Corresponding author. Fax: +81 6 6721 2353.
E-mail address: k_kakehi@phar.kindai.ac.jp (K. Kakehi).

[1] *Abbreviations used:* 2AA, 2-aminobenzoic acid; HPLC, high-performance liquid chromatography; CE, capillary electrophoresis; MS, mass spectrometry; MALDI–TOF, matrix-assisted laser desorption/ionization time-of-flight; GAG, glycosaminoglycan; HS, heparan sulfate; HA, hyaluronic acid; DHB, 2,5-dihydroxybenzoic acid; $NaBH_4$, sodium borohydride; PBS, phosphate-buffered saline; MWCO, molecular weight cutoff; NP–HPLC, normal phase HPLC; MS/MS, tandem MS; CS, chondroitin sulfate.

0003-2697/$ - see front matter © 2011 Elsevier Inc. All rights reserved.
doi:10.1016/j.ab.2011.12.017

this system to an automatic spotter (AccuSpot from Shimadzu) for direct matrix-assisted laser desorption/ionization time-of-flight (MALDI–TOF) MS measurement for routine analysis of *O*-glycans, and the analysis of the released *O*-glycans is completed within 1.5 h [11].

During the releasing reaction, we found that glycosaminoglycans (GAGs) are also conveniently released from proteoglycans. The released GAGs are digested with specific eliminases to produce a mixture of unsaturated disaccharides that are conveniently labeled with a fluorescent tag such as 2AA or 2-aminoacridone and analyzed by CE [12].

These two types of *O*-glycans (mucin-type glycans and GAGs) are concerned with various biological functions [13–16], and there are a number of research works on the aberrant glycan patterns in relation to progression of diseases [17–20]. Structural alterations of mucin-type glycans are often observed in tumors. For example, core 3 and core 4 mucin-type glycans are synthesized in normal cells but apparently down-regulated in gastric and colorectal carcinoma [21,22] (see Supplementary Fig. 1 in supplementary material for the core structures of *O*-glycans). Iwai and coworkers showed that expression of the enzymes related to the synthesis of core 3 structure reduced tumor formation in human fibrosarcoma cells [22]. Cancer-associated mucin-type glycans were highly sialylated but less sulfated and were often truncated [23–25]. Truncated mucin-type glycans such as Tn and T antigens as well as their sialylated analogues became predominant with the progression of cancer [26]. The occurrence of the sialyl-Lewis^x (NeuAcα2-3Galβ1-4(Fucα1-3)GlcNAcβ1-3Gal-R:SLe^x) epitope on *O*-glycans in colon cancer patients is also associated with poor survival [27]. In addition, metastatic cancer cells often express the increased amounts of sialyl-Lewis^a epitope (NeuAcα2-3Galβ1-3(Fucα1-4)GlcNAcβ1-3Gal-R:SLe^a) and SLe^x [28,29].

Many reports on the alterations of GAGs in relation to tumorigenesis have also appeared. Nonsulfated chondroitin is detected in tumor tissues, whereas it is almost absent in normal specimens [30]. Furthermore, differences in the sulfation pattern of heparan sulfate (HS) were also reported [31]. For example, HS from lung cancer cells exhibited a higher degree of oversulfation that was due to an increased content of the three repeating disaccharides having 6-*O*-sulfated glucosamine residues [31]. Highly sulfated HS acts as a coreceptor for a variety of pro-angiogenic factors, such as vascular endothelial growth factor and fibroblast growth factor, and plays vital roles throughout the various stages of angiogenesis and tumor growth [32–34]. Increased levels of hyaluronic acid (HA) are also associated with certain types of human primary and metastatic cancers [35,36]. Vizoso and coworkers measured the expression level of HA in gastric tumor tissues from 129 patients, and they revealed that high expression of HA is an indicator of poor prognosis for patients with gastric cancer [37].

Glycans are not the direct products by genes; rather, they are the product by a combination of actions of the relevant enzymes. Therefore, alteration of structure simultaneously occurs in some glycans, and comprehensive analysis of glycan structures is required to reveal the relationship between biological characteristics and glycans. Two types of these *O*-glycans described above were commonly attached to serine (or threonine) residues on peptides and can be affected with each other. Based on these considerations, determination of alterations of multiple kinds of glycans will lead to accurate understanding of diseases, including tumors.

Unfortunately, it should be noticed that profiles of mucin-type *O*-glycans and GAGs have been reported independently. In addition, there is little information on the relationship between the changes of mucin-type *O*-glycans and GAGs. If we can obtain both types of information at the same time, the amount of knowledge on both glycans can increase dramatically and will be an important tool for cancer diagnostics and therapies. Based on these considerations, this study aimed at one-pot analysis of mucin-type *O*-glycans and GAGs.

Materials and methods

Materials

Pronase (*Streptomyces griseus*) was obtained from Calbiochem (San Diego, CA, USA). 2AA and sodium cyanoborohydride for fluorescent labeling of the released glycans were obtained from Tokyo Kasei (Tokyo, Japan) and Sigma–Aldrich Japan (Tokyo, Japan), respectively. Sephadex LH-20 was obtained from GE Healthcare (Tokyo, Japan). Triton X-100, 2,5-dihydroxybenzoic acid (DHB), and sodium borohydride ($NaBH_4$) were also obtained from Sigma–Aldrich Japan. Protein inhibitor cocktail for animal cells was obtained from Nacalai Tesque (Kyoto, Japan). A serotonin-immobilized column for the separation of sialo glycans was obtained from Seikagaku Biobusiness (Tokyo, Japan). Chondroitinase ABC, heparitinase 1, heparitinase 2, and standard samples of unsaturated disaccharides for the analysis of GAGs were also obtained from Seikagaku Biobusiness. Fused silica capillary tubing (50 μm i.d.) was obtained from GE Healthcare. Other reagents and solvents were of the highest grade commercially available or HPLC grade. All aqueous solutions were prepared using water purified with a Milli-Q purification system (Millipore, Bedford, MA, USA).

Cell cultures

In the current study, human-derived cancer cells were employed: U937 (histiocytic lymphoma), K562 (chronic myelogenous leukemia), Jurkat (acute T cell leukemia), HL-60 (acute promyelocytic leukemia), LS174T (colorectal adenocarcinoma), HCT116 (colorectal adenocarcinoma), HCT15 (colorectal adenocarcinoma), BxPC3 (pancreatic adenocarcinoma), PANC1 (pancreatic carcinoma), and MKN7 and MKN45 (gastric adenocarcinoma). All of these cells except LS174T were cultured in RPMI 1640 medium supplemented with 10% (v/v) fetal calf serum and 1% (v/v) penicillin/streptomycin mixed solution (10,000 U/ml penicillin and 10 mg/ml streptomycin, Nacalai Tesque). LS174T cells were cultured in minimum essential medium supplemented with 10% (v/v) fetal calf serum. Fetal calf serum was previously kept at 56 °C for 30 min. The cells were cultured at 37 °C under 5% CO_2 atmosphere and harvested at 80% confluent state. Collected cells (1.0×10^7 cells) were washed with phosphate-buffered saline (PBS) and collected by centrifugation at 1000 rpm for 20 min.

Glycopeptide pool from whole cells

Glycopeptide pool derived from cancer cells was prepared according to the method reported previously [38]. Cultured cells (1.0×10^7 cells) were suspended in 5 mM Tris–HCl buffer (pH 8.0, 500 μl) and mixed with an equal volume of 2% Triton X-100 in the same buffer in an ice bath. After homogenizing the cells for 7 min with a glass homogenizer, the mixture was centrifuged at 8000*g* for 30 min. The supernatant layer was collected and boiled for 7 min at 100 °C and evaporated to dryness by a centrifugal evaporator (SpeedVac, Savant, Sunnydale, CA, USA). The lyophilized material was suspended in water (200 μl), and ethanol (800 μl) was added to the mixture to 80% concentration. The precipitate was collected by centrifugation and washed with ethanol (1 ml × 3) and then with acetone (1 ml × 2), followed by drying in vacuo. The residue was digested with pronase (50 μg) in 50 mM Tris–HCl (pH 8.0, 200 μl) at 37 °C for 24 h. The reaction mixture was boiled for 10 min, and the supernatant was collected after centrifugation. Because free glycans present in some cancer cells inhibit the subsequent analysis of *O*-glycans [39], reduction